NIR studies of the interactions of decatungstate triplet with various organic molecules

Anastasiia Suprun

Thesis submitted to the University of Ottawa
in partial Fulfillment of the requirements for the
Master of Science Chemistry

Department of Chemistry and Biomolecular Sciences
Faculty of Science
University of Ottawa

Supervisor: Juan (Tito) Scaiano

Abstract

The work presented in this thesis was carried out at the Department of Chemistry & Biomolecular Sciences, University of Ottawa, Canada. It primarily addresses the hitherto unexplored photochemistry of decatungstate (DT) using a laser-based time-resolved techniques. As a member of the polyoxometalate family, the DT anion has attracted a lot of attention for the purpose of photocatalytic C–H functionalization. This is due to its remarkable photochemical activity, which holds great promise for future applications in photochemistry.

Firstly, based on the extensive literature survey, a basic introduction to photochemistry related to DT, hydrogen atom abstraction reaction, and the role of DT in photocatalysis is provided. Details of the experimental techniques and instruments involved in the research work are also given.

A detailed investigation characterizing the triplet state of decatungstate with a laser-based technique by studying the near-infrared emission is presented. The discovery of near-infrared (NIR) phosphorescence with a lifetime of around 100 ns, from the transient described as wO allows its unequivocal identification as the triplet state of DT in acetonitrile. Quenching of triplet DT with various hydrogen donors is also studied, and the rates are determined, allowing an understanding of the role of DT as a catalyst. Our results explain hitherto unclear phenomena, i.e., the absence of oxygen quenching of decatungstate triplet (^{3}DT*).

Further, to understand the role of DT as a photocatalyst, the quenching behaviour of the first excited triplet state of decatungstate (DT) using various peroxides, namely cumene hydroperoxide, tert-butyl hydroperoxide, and hydrogen peroxide, is examined and compared.

Acknowledgements

I express my deepest gratitude to Prof. Juan (Tito) Scaiano, whose unwavering support and guidance have been invaluable throughout my Master's journey. In July 2022, when I arrived in Canada from Ukraine during the challenging times of the war, Prof. Scaiano not only accepted me into his research group as a master's student but also generously provided me with a scholarship. His kindness and willingness to help have left a lasting impression on me.

Throughout my master's course, Prof. Scaiano has been a constant source of encouragement and knowledge. His dedication to his students and his field is truly inspiring. Prof. Scaiano has consistently supported me in my academic and personal growth.

I am very grateful for the opportunity to study and work under his guidance, which played an important role in my academic and personal development. His mentorship helped me improve my research skills and cope with the challenges of studying during a difficult time in my life.

Thank you, Tito, for believing in me and for all you have done to make my academic journey successful and memorable. Your support has helped me succeed academically and fostered personal growth and resilience that I will carry with me throughout my career.

I also want to personally thank to Saba Didarataee who I was working with on the part of the DT project, and Neeraj Joshi who taught me everything I know about the laser systems. As well I want to thank you to the rest of Scaiano group. Discussions on various scientific topics with my colleagues from the research group have helped me enormously, and I thank them for inspiring discussions and

their ever-helpful attitude. I am thankful for the pleasant company I have experienced during my studies. They always come up with suggestions, consolation and encouragement, whichever is needed in academic and personal matters during good and hard times.

Last but not least, I would like to express my deepest gratitude to my mom, Svitlana, who brought me to Canada after the war in Ukraine started and helped my brother and me settle here, to my father Volodymyr and younger brother Yaroslav for their continuous support, patience and encouragement. Without them I wouldn’t be able to get my MSc degree. Thank you!

Table of Contents

List of Figures

List of Tables

List of Abbreviations

[]	Concentration
$^1O_2$	Singlet oxygen
^{3}DT*	Decatungstate triplet
ACN	Acetonitrile
DT	Decatungstate
DTH•	Reduced form of decatungstate
Fl	Fluorescence
HAT	Hydrogen atom transfer
HOMO	Highest occupied molecular orbital
HPAs	Heteropolyanions
hν	Light
IC	Internal conversion
ISC	Intersystem crossing
IVR	Intramolecular vibrational relaxation
IPA	Isopropanol
IPAs	Isopolyanions
kQ	Rate constant
LFP	Laser flash photolysis
LMCT	Ligand to metal charge transfer

LUMO	Lowest unoccupied molecular orbital
MO	Molecular orbital
Nd:YAG	Neodymium-doped yttrium aluminum garnet
NIR	Near infrared
pK	Negative logarithm of the dissociation constant K (-logK)
PCET	Proton-coordinated electron transfer
Ph	Phosphorescence
PMT	Photomultiplier tube
POMs	Polyoxometalates
RB	Rose bengal
RH	Substrte
ROS	Reactive oxygen species
S_0	Ground state
S_1,S_2	Singlet exited states
SET	Singlet electromtransfer
T_1,T_2	Triplet exited states
TA	Transient absorption
TBADT	Tetrabutylammonium decatungstate

TFA	Trifluoroacetic acid
THG	Third harmonic generator
TEA	Triethylamine
UV	Ultraviolet
Vis	Visible
wO	Decatungstate intermediate
$[W_{10}O_{32}]^{4-}$	Decatungstate anion
$[W_{10}O_{32}]^{5-}$	One-electron-reduced form of decatungstate
$\boldsymbol{f}_{Q}$	Fraction quenched
$\boldsymbol{\Phi}_{R}$	Quantum yield
ΔOD	Change in optical density

Chapter 1: Fundamentals of photochemistry as applied to decatungstatechemistry

1.1 Opening remarks

This chapter is focused on the principle and theories of the photochemistry related to the investigation carried out in the thesis. When a molecule transitions to an electronic excited state through photon absorption, it exhibits distinct chemical and physical characteristics compared to its initial ground state, effectively transforming into a unique chemical entity with altered properties. The chemical and physical properties of a molecule vary between its excited state and ground state. Certain physical properties like dipole moment, pK values, redox potentials and polarizabilities also differ in the excited state. Following the absorption of light, the excited molecule may relax with radiative or by means of variety of non-radiative processes or may undergo a chemical transformation in form of a stable product. This chapter also describes the basic principle of hydrogen atom transfer (HAT) and electron transfer reaction and decatungustate as photocatalyst for HAT reaction.

1.2 Lambert-Beer's Lawand Absorbance

The rate of absorption can be determined using the Lambert-Beer law. It can be expressed as[1]:

$$A = \varepsilon lc \qquad (1)$$

Where: A - is the absorbance at a particular wavelength; ε - is the molar extinction coefficient; l - is the optical path; c - is the concentration of the absorbing species;

Usually the spectrum is a plot of light transmitted against wavelength, but chemist prefer to use absorbance because it's connected to concentration. Absorbance is connected to transmittance (T) by expression:

$$A = -logT \qquad (2)$$

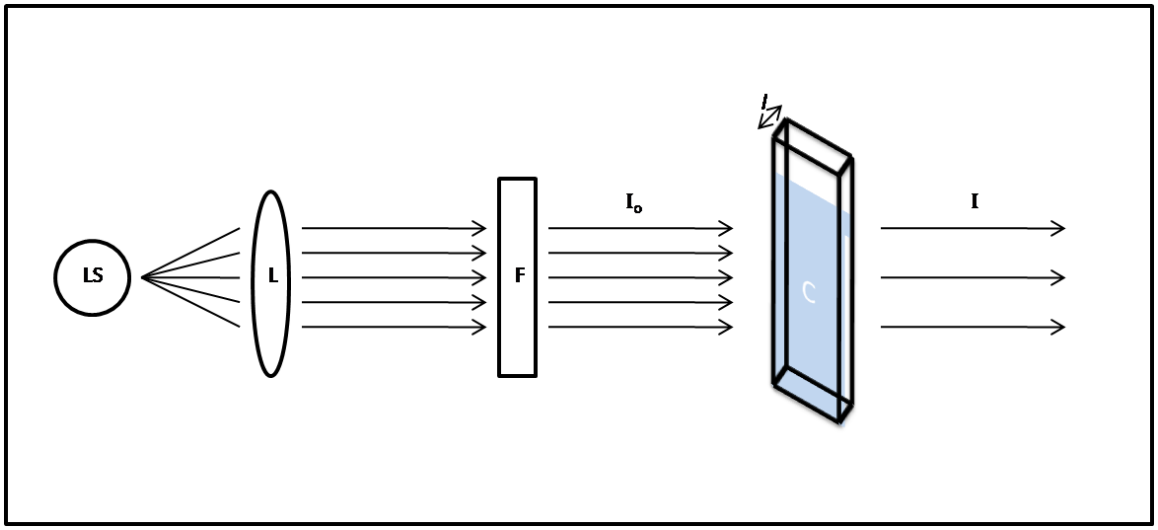

Figure 1.2.1: Optical arrangement for measuring absorbance by a collimated beam of radiation. LS = light source, L = lens, F = filter, C = sample cell, l = optical path length, I0 = incident light intensity, I = transmitted light intensity.

When there is more than one absorbing species in the solution, which don't interact with each other, assuming path length to be same, the measured total optical density (*OD*)for the solution is[1]:

$$OD = OD_1 + OD_2 + OD_3 + \ldots\ldots\ldots \qquad (3)$$

1.3 Types of electronic transition in organic molecules

When a molecule absorbs UV-vis radiation, it undergoes electronic excitation, causing an electron to move from its electronic ground state to a higher energy state, typically transitioning from the Highest Occupied Molecular Orbital (HOMO) to the Lowest Unoccupied Molecular Orbital (LUMO) (Figure. 1.3.1).

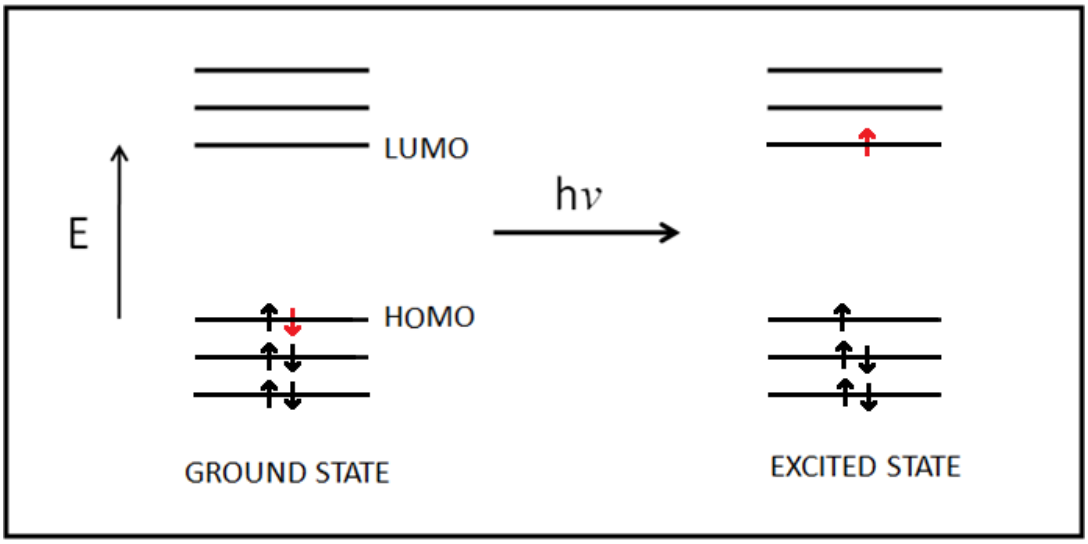

Figure 1.3.1: Electronic transition from HOMO to LUMO, including the change of the spin

Electronic transition typically originates from valence electrons within a molecule, known as the chromophore, comprising nonbonding (n) or π-electrons. These transitions are categorized into various types based on the molecular orbital they involve, such as n →π*, π→π*, n →σ*, σ→σ*, and σ→π* (Figure1.3.1). These transitions appear in certain regions of the electromagnetic spectrum. The shifts associated with n →π* and π→π* commonly detected in the UV-visible regions of organic compounds[1].

When all bonding orbitals are repeatedly occupied in their state, the Pauli principle indicates a singlet state, but when excitation occurs, the electrons are separated into orbitals and the spin restrictions are relaxed. Then both singlet and triplet states are possible[1].

Thus, in organic molecules, the potential shared energy levels include $^{1}(n, \pi^*)$, $^{3}(n, \pi^*)$, $^{1}(\pi, \pi^*)$ and $^{3}(\pi, \pi^*)$ which are determined by the characteristics of the molecule itself (Figure 1.3.2).

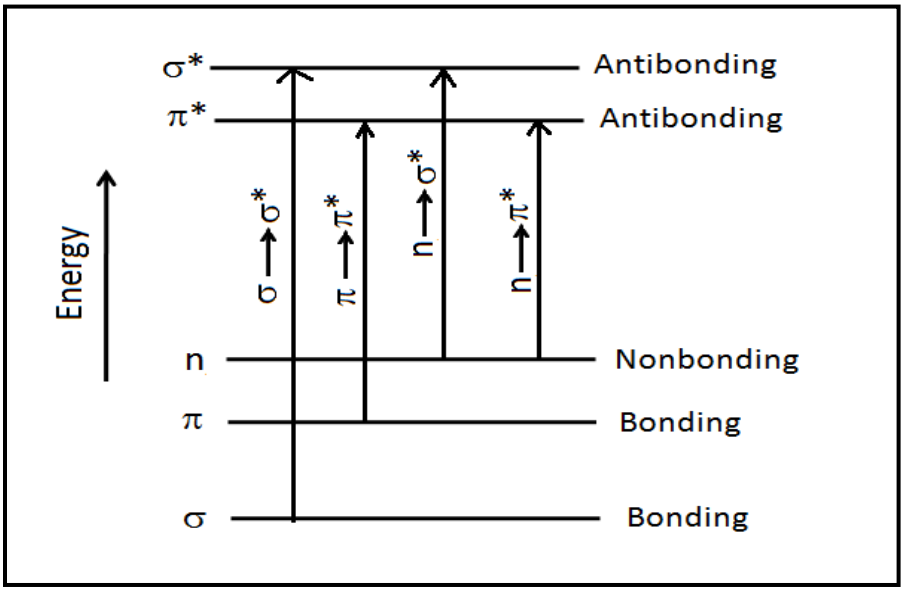

Figure 1.3.2: Different electronic transitions according to the molecular orbital involved.

Hund's rule states that the lowest-energy excited state is the triplet state. In Jablonski diagrams (Figure 1.3.3), singlet levels are usually depicted on the left as horizontal lines, forming each other above the sequences of energy levels, and triplet levels are slightly shifted to the right.

The initial energy state of a system is referred to as the ground state and is assigned a zero-energy value. A Jablonski diagram (shown in Figure 1.4.1) is a useful tool for representing various photophysical and photochemical

processes which may take place after radiation absorption. We will discuss this diagram in detail later.

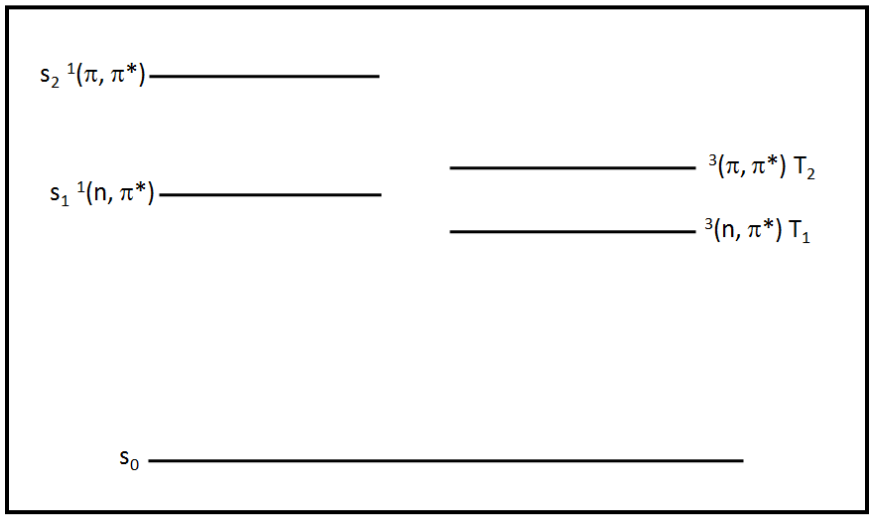

Figure 1.3.3: Energy level diagram for (n, π*) and (π, π*), singlet and triplet states.

1.4 Jablonski Diagram

The after light absorption processes are usually described using the Jablonski diagram, which serves as the main tool for explaining the phenomena of absorption and emission of light.

This diagram is used in a variety of formats to describe the many molecular interactions possible in excited states. In the diagram, the ground singlet state and the first and second electronic states are denoted as S_0, S_1 and S_2, respectively, and the initial triplet electronic state is denoted as T_1. At each of these electronic energy levels, fluorophores can occupy different vibrational energy levels, designated 0, 1, 2, etc[2].

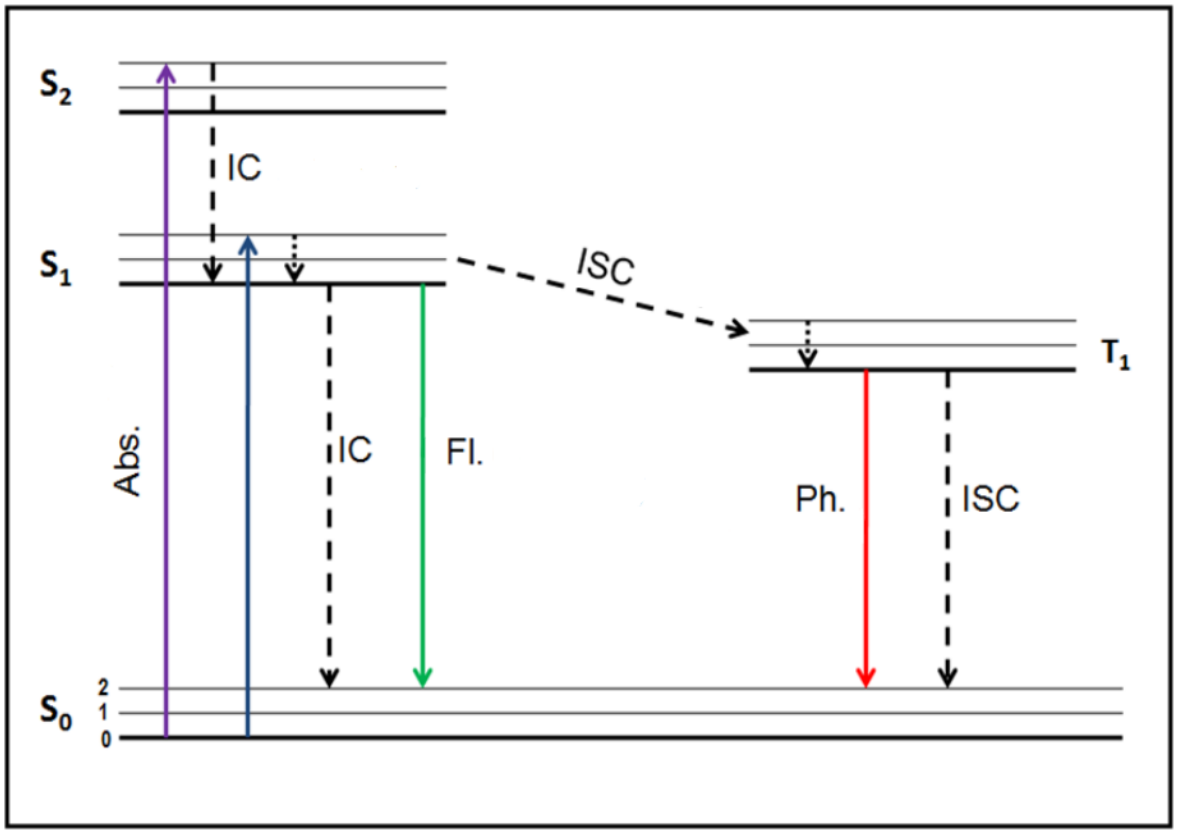

Figure 1.4.1: Jablonski diagram: Abs – absorption; IC – internal conversion; ISC - intersystem crossing; Fl – fluorescence; Ph – phosphorescence.

When a molecule becomes excited, it releases energy through radiative and non-radiative processes. Radiative processes involve the molecule returning from a higher to a lower electronic state by emitting a photon, which is known as luminescence. Luminescence can be divided into fluorescence (relaxation from higher energy state to the ground state, a transition between the states of same multiplicity) and phosphorescence (relaxation from higher triplet energy state to the singlet ground state, a transition between the states of different multiplicity). Non-radiative transitions can occur through internal conversion (IC) and intersystem crossing (ISC). IC occurs between energy states of the same spin multiplicity, while ISC occurs between energy states of different spin multiplicity.

Large polyatomic molecules dissipate energy through intramolecular vibrational relaxation (IVR), while in small molecules, collisional interaction may lead to relaxation. The surrounding environment (solvent medium) acts as a heat bath. The molecule may cross to a different electronic state by IC or ISC. ISC is responsible for populating the triplet state, and the emission from triplet to singlet appears as phosphorescence. In most cases, emission takes place exclusively from the lowest vibrational level of first excited singlet state (Kasha's rule)[2].

1.5 Lifetime (decay time) of excited electronic states of molecules

By absorbing a quantum of radiation, an electron moves to a higher energy level, which makes us wonder how long its excited state will last before returning to a stable ground state. In systems consisting of many molecules, the rate of decay obeys a first-order rate law and can be expressed as[1]:

$$I = I_0 e^{-k_r t} \qquad (4)$$

Where I_0 and I are intensities of the emitted radiation at zero time and at any time t after the exciting radiation is cut off respectively; k_r is the rate constant for the emission process and has the dimension of reciprocal time.

If

$$k_r = \frac{1}{\tau_0}, then\ I = I_0 e^{-t/\tau} \qquad (5)$$

At $t = \tau$,

$$I = \frac{I_0}{e} \quad (6)$$

Therefore, the lifetime is the duration required for the intensity to decrease to 1/e of its original value.

1.6 Photo-induced hydrogen atom transfer (HAT)

Hydrogen atom transfer (HAT) is a common one-step reaction that involves the transfer of a proton and an electron between two substrates or molecules. The overall HAT reaction is shown in Equation (7).

$$A_1H + A_2^{\bullet} = A_1^{\bullet} + A_2H \quad (7)$$

HAT is a key step in many organic reactions such as aerobic oxidation, hydrocarbon combustion, enzymatic catalysis or atmospheric processes. HAT reactions are widely studied by various research groups that study the mechanisms of HAT in various substrates as well as the rates of their reactions. Quite a few HAT reactions occur via the alternative proton-coordinated electron transfer (PCET) pathway. It involves the abstraction of a proton by the atomic center of the abstractor molecule and at the same time the transfer of an unpaired electron through an orbital that does not participate in the bond creation[3].

HAT reactions are divided into direct and indirect. Direct HAT describes HAT in which the excited photocatalyst directly carries out the HAT. Such photocatalysts include ketones in the triplet state or decatungstate photocatalysts. Hydrogen atom transfer reactions provide great advantages in organic synthesis, allowing the activation of aliphatic C-H bonds with high selectivity. In this way, reaction conditions can be easily adjusted

without introducing directing or protecting groups into the substrates. Recently, photocatalysis has become increasingly used. In this case, the excited catalyst initiates the start of the reaction, forming reactive intermediates from the reactants, and then returns to its normal state.

The direct HAT method is based on the ability of the excited state of the photocatalyst to directly remove a hydrogen atom from the substrate (Figure 1.6.1.a). In indirect HAT, the radical abstractor of the hydrogen atom is generated in situ. Photocatalyst can generate a thermal hydrogen abstractor by interaction with a suitable species. A reverse hydrogen atom transfer which undergoes the energy transfer from the photocatalyst to the substrate can occurs leading to formation of thermal hydrogen abstractor which abstracts hydrogen from the molecule(Figure 1.6.1.b). The photocatalyst can promote proton-coupled electron transfer (PCET) with the participation of an appropriate base, which leads to the formation of a radical that abstracts a hydrogen atom from the substrate (Figure 1.6.1.c). Alternatively, a sequential electron/proton transfer mechanism may occur. First, the photocatalyst can cause a single electron transfer (SET) to create a radical ion, which either directly abstracts a hydrogen atom from the substrate or loses a charge to form a hydrogen radical (Figure 1.6.1.d)[3].

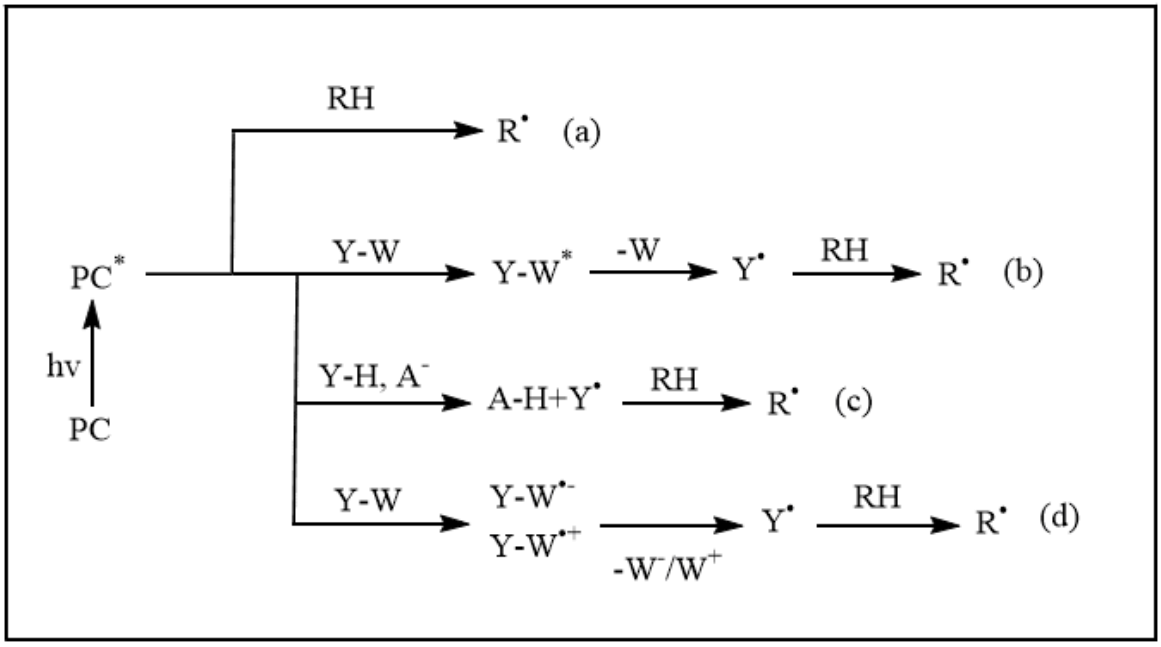

Figure 1.6.1: Activation of the substrate by hydrogen atom transfer (HAT) facilitated by either a direct (a) or indirect: (b) – Energy transfer; c – Proton-coupled electron transfer; d – Singlet-electron transfer).Ref.[3]

The range of photocatalysts that are capable of reacting via the direct HAT mechanism is not very large. These mainly include polyoxometalates such as the decatungstate anion $[W_{10}O_{32}]^{4-}$ or the uranyl cation $[UO_2]^{2+}$. They also include aromatic ketones. Highly electrophilic oxygen centers, which imitate the behavior of an alkoxy radical, are responsible for the reactivity.

Since its discovery, the decatungstate anion has been widely used in various photocatalytic synthetic processes aimed at activating organic substrates through the hydrogen atom transfer, for example, for the formation of C–C[4–9], C–O[10], C–N[11,12], C–S[13], C–D[14]and C–halogen bonds[15,16], fluorination reactions[17], dehydrogenation[18,19] and others.

1.7 Laser Flash Photolysis (LFP)

The flash photolysis method was introduced in 1949 by Manfred Eigen, Ronald George Norrish and George Porter, who won the Nobel Prize in Chemistry in 1967. The LFP technique is used to study transient species generated during photo-induced reactions by measuring the absorption of transient species. After light is absorbed by a molecule or material, the resulting photophysical and photochemical reactions occur quickly, taking only femtoseconds to a few microseconds. Pulsed laser systems are an excitation source that enables the real-time investigation of photophysical and photochemical reactions[20]. The typical LFP setup is shown on Figure 1.7.1.

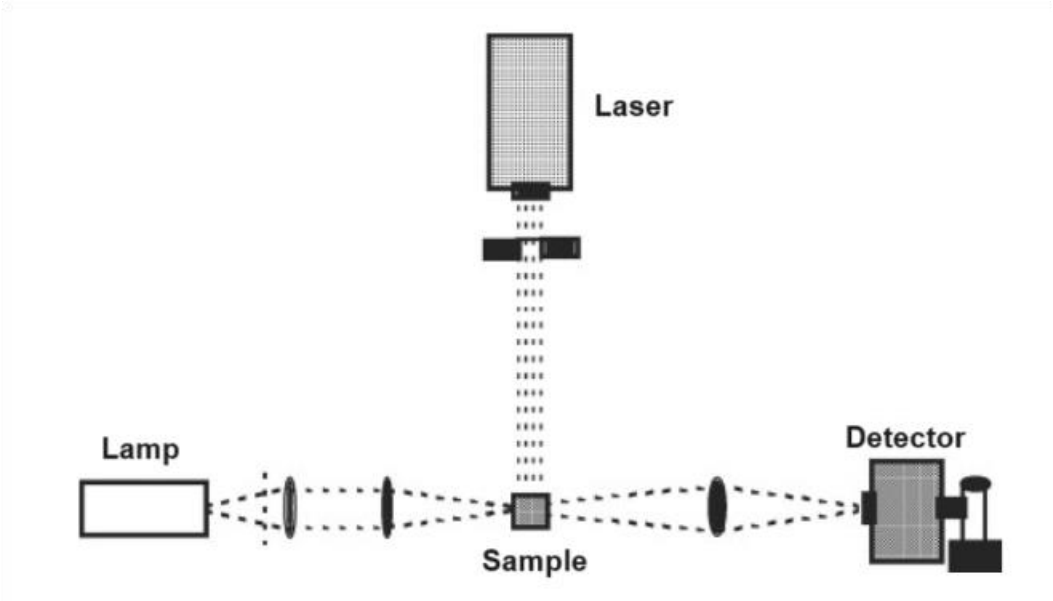

Figure 1.7.1: Typical LFP system. Reproduced from ref[20] with permission. Copyright © 2004 John Wiley & Sons, Inc.

Under normal conditions, molecules in a solution tend to remain in their ground state with minimal energy. However, when a photon is absorbed, it

boosts the molecule's energy by promoting one of its electrons to a higher orbital. Following this excitation, the molecule can return to its ground state through several intermediate stages, including singlet and triplet excited states, or it might undergo a photochemical reaction. In either case, the excited and transient states display unique absorption spectra, which can be tracked by observing alterations in absorption at specific wavelengths.

Pulsed excitation through flash photolysis allows for the monitoring of rapid reactions, enabling a thorough reconstruction of the entire reaction pathway. The initial flash induces the formation of a notable population of intermediates in the sample, which subsequently absorb light from the laser flash. This absorption correlates with the concentration of the intermediates according to the Lambert-Beer law. Changes in absorption spectra over time can elucidate alterations in the concentration of photoinduced intermediates and, thus, the kinetics of the processes involved. However, flash photolysis is limited to transparent samples. For opaque samples the diffuse reflectance is used.

In order to understand the process that occurs during the LFP experiment, let’s look on the example of an excited triple state. Illustrated in Figure 1.7.2 is an energy diagram depicting a species being stimulated to the S_1 state by a laser pulse, subsequently transitioning to the triplet T_1 state through intersystem crossing. The duration of the triplet state can be determined by its phosphorescence lifetime. Monitoring the signal post-laser excitation enables the tracking of changes in T_1 phosphorescence over time as the population of the excited state diminishes from T_1 to the ground state S_0, leading to a corresponding reduction in phosphorescence levels. The signal

from the LFP is normally a plot of the optical density(ΔOD) versus time at a given wavelength. The intensity of the signal depends on different parameters[21].

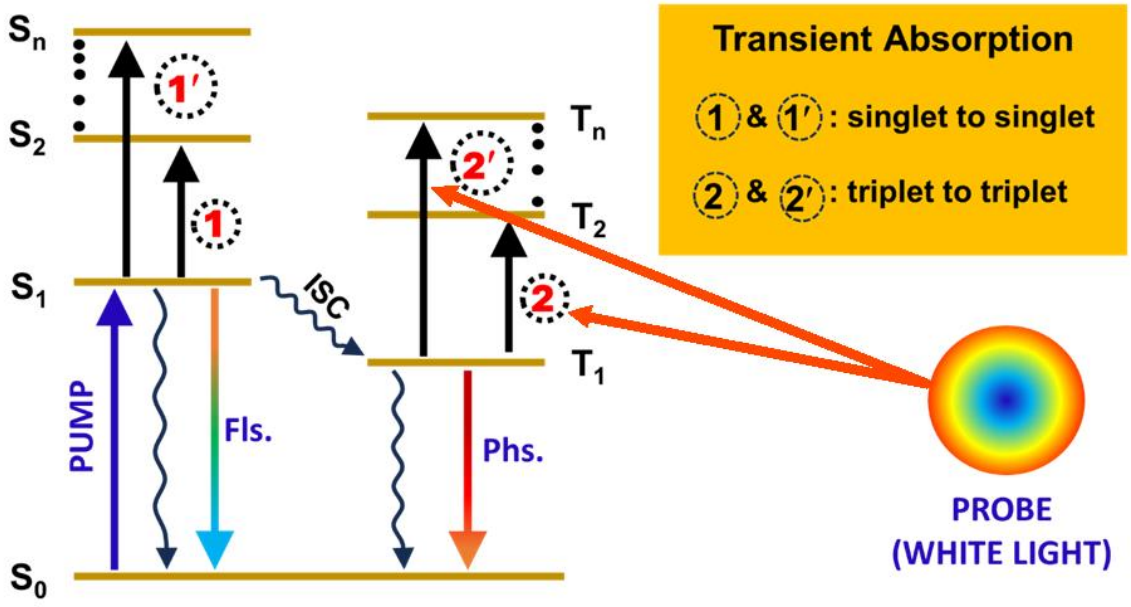

Figure 1.7.2: Schematic energy diagram for transient absorption of a triplet states, with a pump laser (blue) and white light probe (red).

The signal intensity depends on the pulse energy delivered by the laser, but if the laser intensity is too high then other problems associated with very high laser doses may arise. Absorbance is independent of light monitoring intensity. However, if the light intensity is too high, noise may appear that distorts the signals. As well, many reactive intermediates can decompose through self-reactions. In such cases, it is better to stick to low concentrations to minimize adverse reactions.

1.8 Polyoxometalates (POMs)

Recently, a lot of attention has been given to the study of polyoxometalates. These cluster compounds exhibit unique properties that are useful in different fields such as catalysis, photocatalysis, electrocatalysis, development of energy carriers, research of supramolecular and self-assemblies, and the creation of drugs for fighting viruses and cancer.

The first phosphomolybdate $[PMo_{12}O_{40}]^{3-}$ was reported by Berzeliusin in 1826, which initiated the chemistry of polyoxometalates (POM). Subsequently, Marignac identified two isomeric forms of $[SiW_{12}O_{40}]^{4-}$, and Keggin elucidated the structure of $[PW_{12}O_{40}]^{3-}$ in the early 1930s. These early discoveries laid the foundation for the synthesis and characterization of numerous POM structures[22].

Polyoxometalates (POMs) are molecular oxides that are formed by a combination of oxygen and early transition metals such as V, Nb, Ta, Mo, and W at their highest oxidation states. They can also include a variety of heteroatoms such as P, As, Si, and Ge. POMs are different from most metal oxides as they can have a range of tens to hundreds of metal atoms in a single cluster molecule, forming nanoparticles[23].

POMs are 4-fold- or 6-fold-coordinated and lie in the center of the M_xO_y shell. Depending on the presence of atoms other than oxygen and transition metals, two types of POM species can be identified[24]:

Isopolyanions (IPAs) $[M_nO_y]^{p-}$

Heteropolyanions (HPAs) $[X_zM_nO_y]^{q-}$, with $z \leq n$

Polyoxometalates (POMs) are stable under irradiation, which makes them excellent photocatalysts. Decatungstate is a member of the POM family, it's often used as sodium or tetrabutylammonium salts (Scheme 1.8.1). While other POMs find applications in different fields, decatungstate is widely used as photocatalyst due to its exceptional reactivity[25].

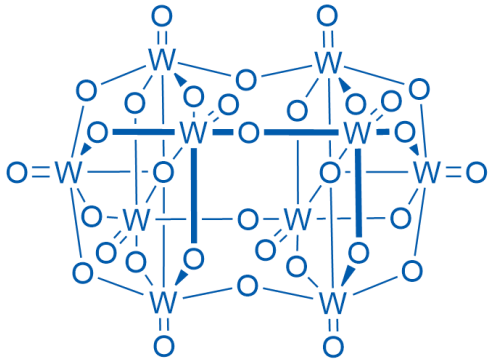

Figure 1.8.1:The structure of decatungstate (DT)

1.9 Decatundstate photocatalysis

Hill et al.[26]and numerous other groups[27,28] have extensively studied the DT excited state dynamical behavior in the condensed phase using nanoseconds to femtoseconds transient absorption spectroscopy, yielding a comprehensive understanding of its photo-reaction network.

There is consensus on the fundamental aspects of its mechanism, in particular, the lowest-energy transition leads to the occupation of an excited state denoted as $[W_{10}O_{32}]^{4-*}$, which fast decays to intermediate called as "wO". The $[W_{10}O_{32}]^{4-*}$ species is formed by intramolecular O-to-W ligand to metal charge transfer (LMCT) and exists around 10 ps. The wO is a great hydrogen atom abstractor and react with many different molecules creating

the one-electron redused form. Figure 1.9.1 summarizes the photoreaction network of DT[28].

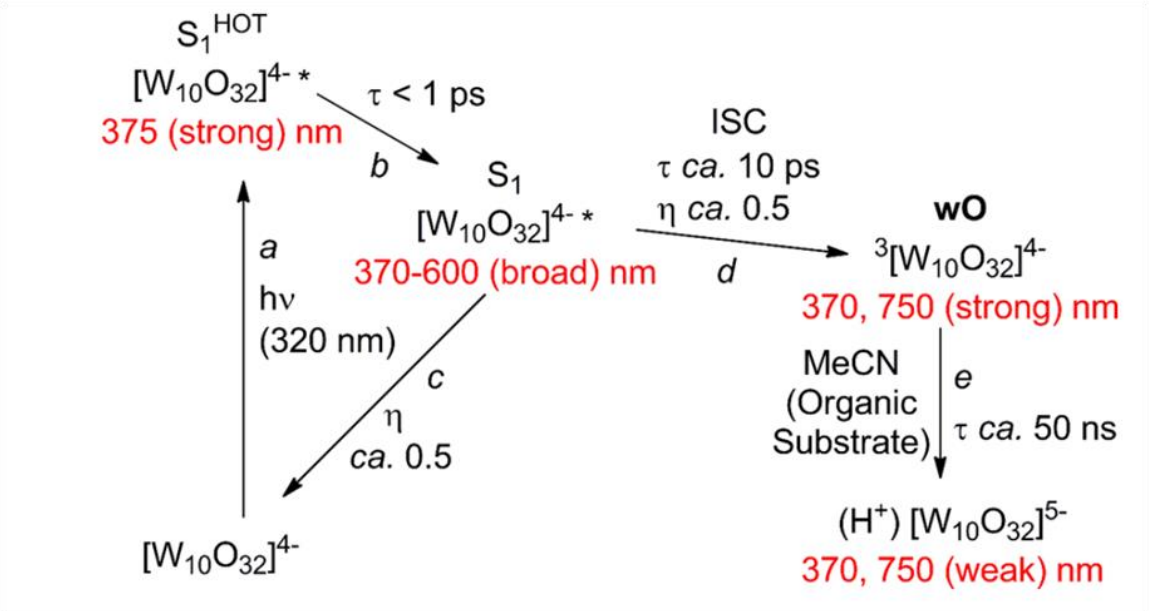

Figure 1.9.1: Absorption regions for each state are marked in red letters. a: photoexcitation and the population of a hot S_1 state, b:evolution of relaxed S_1(geometry minimum), c: S_1 depopulation (ground state recovery), d:S_1 depopulation with the formation of a new state, wO, e:wO interacts with the solvent acetonitrile and led to the mono-reduced form $(H^+)[W_{10}O_{32}]^{-5}$, ref[29].Copyright © 2016 American Chemical Society**.**

The wO species is highly electrophilic and displays partial radical character on the oxygen center. Its predicted redox potential E (wO/$[W_{10}O_{32}]^{5-}$) is around +2.44 V[17]. Depending on the redox properties of the substrate, it can undergo two different types of reactions. On one hand, when the substrate possesses an oxidation potential exceeding +2.44 V, hydrogen-atom transfer (HAT) may take place, leading to the formation of a radical intermediate. On the other hand, if the substrate has an oxidation potential of less than or equal to +2.44 V, then a single-electron transfer (SET) event may occur, leading to the formation of a radical cation (Figure 1.9.2). The oxidation

process leads to the formation of a reduced decatungstate, which can be either protonated or not. In first case the one-electron reduced form (DTH•) particle is formed, and it has a very characteristic blue color. Then, reduced form can regenerate the catalyst back, or it can undergo disproportionation, resulting in the formation of a further reduced and oxidized form[17].

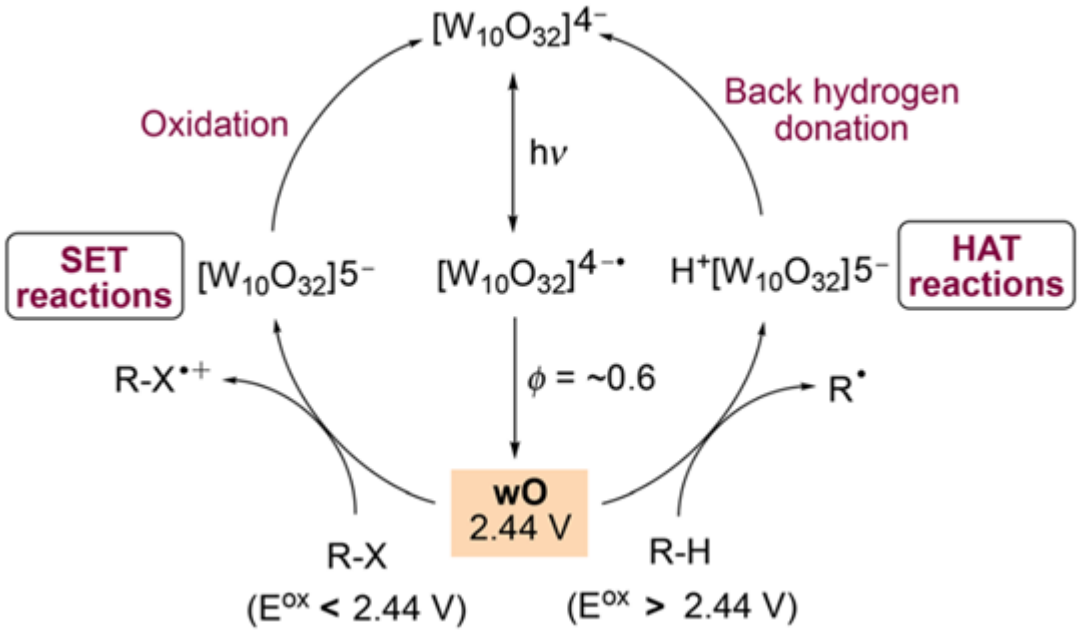

Figure 1.9.2: The structure of decatungstate anion and its photocatalytic cycle which includes single electron transfer (SET) and hydrogen atom transfer (HAT) pathway. Adopted with permission from ref[17]. Copyright © 2023 Royal Society of Chemistry.

The HAT process in decatungstate catalysis shows good site-selectivity. Fagnoni and colleagues have extensively investigated polar and steric effects in decatungstate photocatalysis on the example of C-H bound fictionalization (as shown in Figure 1.9.3). Polar effects control the breaking of C-H bonds and are influenced by highly electrophilic oxygen centers present in tungstate anions that are radical in nature. Steric effects affect site

selectivity in transition states, and in this case they are important due to the large size of the decatungstate anion[30,31].

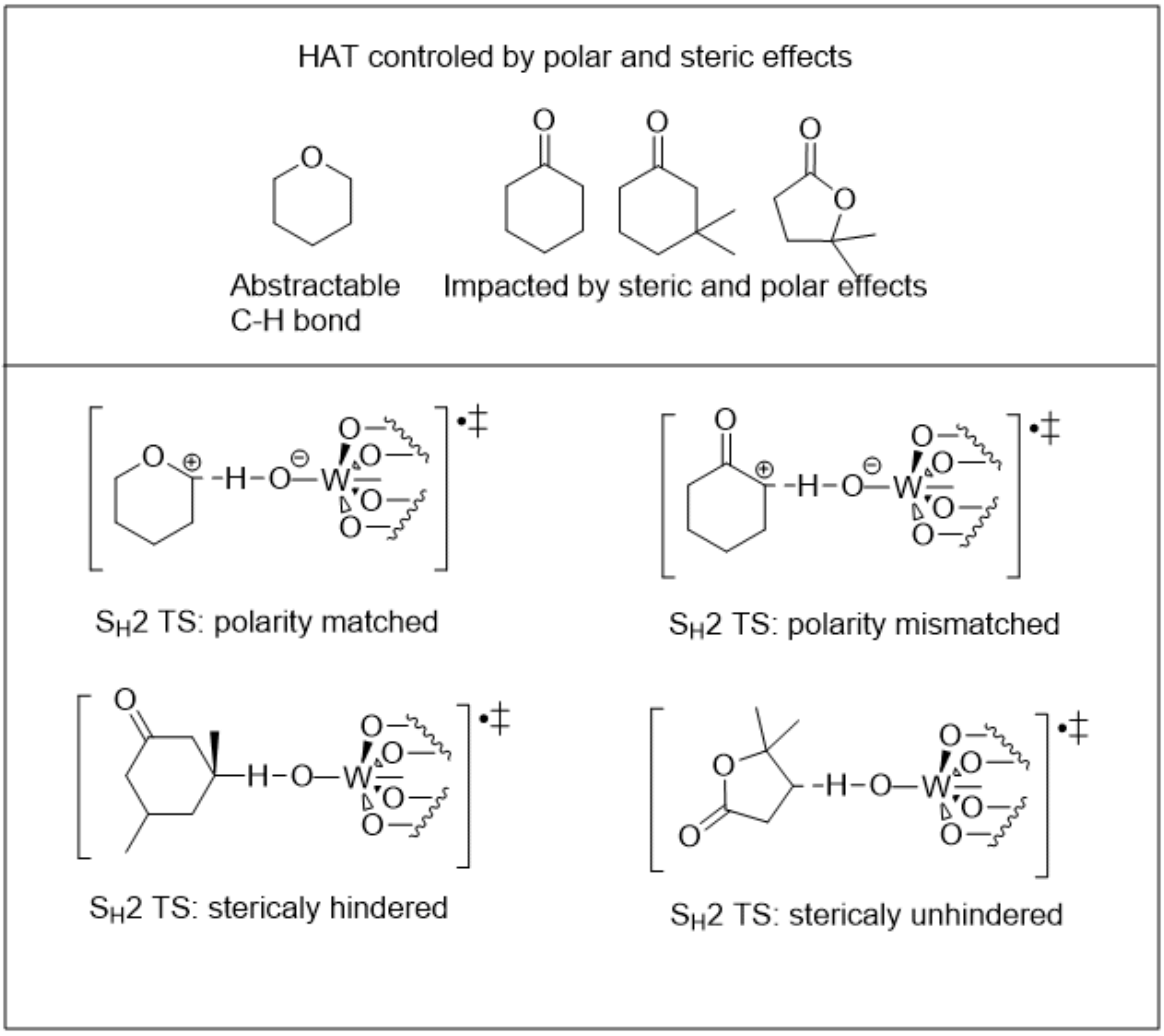

Figure 1.9.3:HAT in decatungstate controlled by polar and steric effects (S_H2: homolytic bimolecular substitution; TS: transition state). Ref[31].

The absorption spectrum of the decatungstate anion ($W_{10}O_{32}^{-4}$) is centered around 324 nm, with absorption band disappearing around 420 nm (Figure 1.9.4)[26].

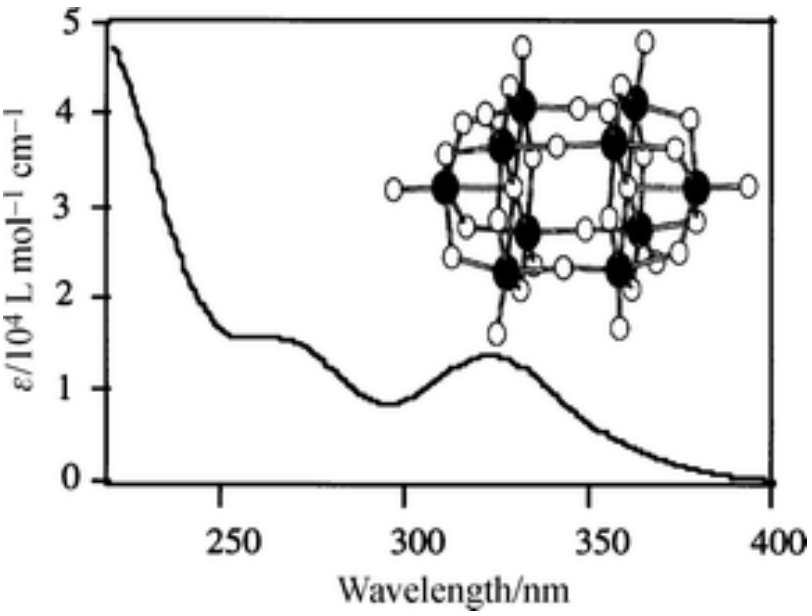

Figure 1.9.4: Structure and absorption spectrum of the decatungstate anion in acetonitrile. Reproduced from ref[32] with permission from the Royal Society of Chemistry.

The decatungstate anion $[W_{10}O_{32}]^{4-}$ demonstrates effective photocatalytic properties under ultraviolet (UV)light[10,17,25,31,33–35]. The primary excited state created after the absorption of a UV photon by sodium or tetrabutylammonium decatungstate is chemically unreactive and decays approximately in 30 picoseconds. However, the initial excited state quickly decays to produce an intermediate that absorbs strongly around 780 nm and exists for around 55 ± 20 ns in acetonitrile (ACN)[28] and 37 ns in water[36].

Yamase demonstrated the formation of a blue species having λ_{max} ~ 630 nm[37] (Figure 1.9.5).The ion $[W_{10}O_{32}]^{4-}$ can accept up to two electrons in long-term photolysis[38]. During the duration of the photoflash, a blue particle exhibiting a λ_{max} = 780 nm emerged and underwent partial decay with a half-life of approximately 1 ms. At longer irradiation times under deaerated conditions, a new band appeared at 630 nm, which corresponds to much

longer lived species. In presence of water (solvent mixture ACN:H_2O with 1:1 rate) this species was not observed.

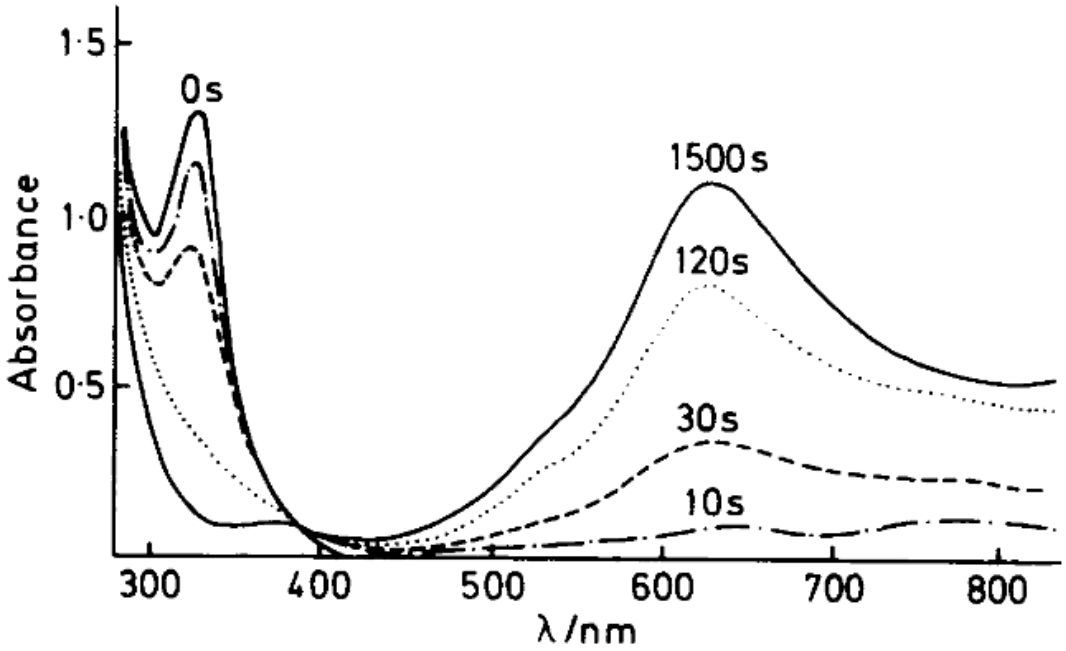

Figure 1.9.5: Absorption spectra of a deaerated solution containing 9.5 x 10^{-5} mol dm^{-3} tetrabutilammonium decatundstate (TBADT) in CH_3CN upon irradiation with 365nm light at room temperature. Times (s) are indicated on the curves. Reproduced from ref[37] with permission from the Royal Society of Chemistry.

Later Tanielian established that the formation of this species is proportional to wO decay. The long-lived nature of this particular species undergoes degradation through second-order kinetics, with an initial half-life lasting 700 nanoseconds. The existence of minimal amounts of O_2 reduces the productivity of this long-lived species and shortens its lifetime. Oxygen appears to prevent the creation of long-lived species by competing and reacting with it[28].The one-electron-reduced form and the two-electron-

reduced form, can be easily identified by their visible spectra, by characteristic peaks at 780 and 635 nm, respectively[39].

The assumption that this long-lived species could potentially be produced through electron transfer was formulated based on the similarities observed in the absorption spectrum of this entity to those of the one-electron-reduced form of decatungstate. ACN can exist in reduced form (CH_3CN^-), which decays quickly at a rate constant of $3.5x10^5$ s^{-1}. However, in the presence of decatungstate the decay rate of CH_3CN^- is accelerated and the one-electron-reduced form of decatungstate ($[W_{10}O_{32}]^{5-}$) is produced with a rate constant of $5.5\times10^9 M^{-1}s^{-1}$.[28] $[W_{10}O_{32}]^{4-}$ creates a complex with the solvent due to which the oxygenation of acetonitrile occurs[40].

More reactive substrate is propan-2-ol. The addition of increasing amounts of propan-2-ol into an acetonitrile solution containing decatungstate leads to a rise in the production of the one-electron-reduced species with a reaction rate constant of 1×10^8 $M^{-1}s^{-1}$. (Figure 1.9.6)[24].

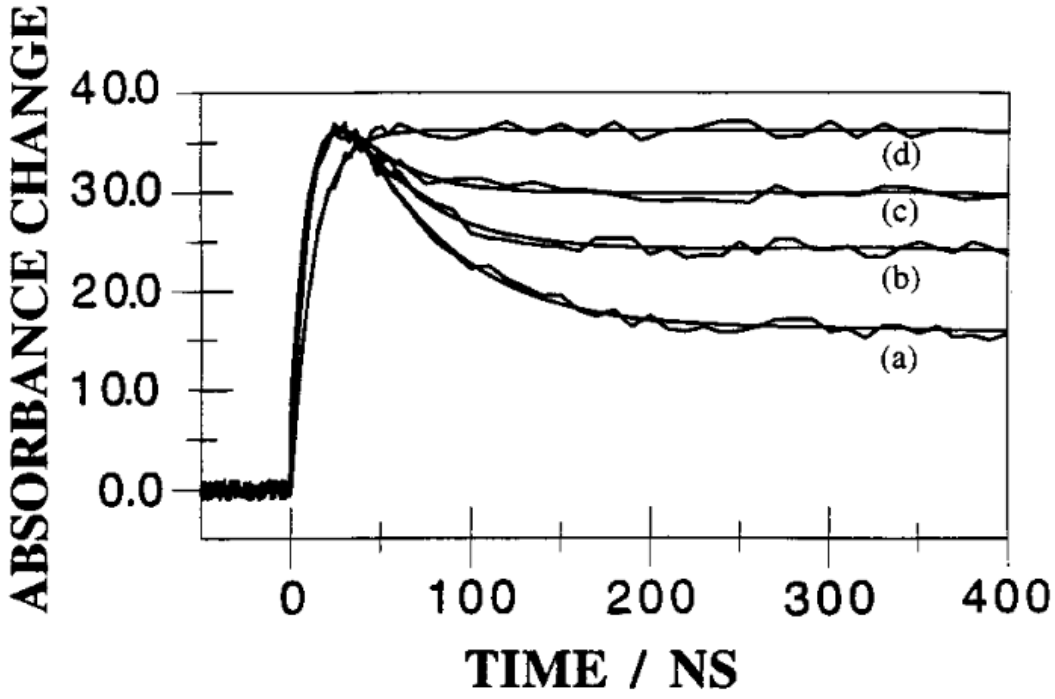

Figure 1.9.6: Effect of propan-2-ol [XH] on the decay of wO in an air-saturated acetonitrile solution of 5×10^{-4} M tetrabutylammonium decatungstate observed at 760 nm following 355 nm excitation with a 15 ns laser pulse: (a) [XH] = 0.01 M, (b) [XH] = 0.10 M, (c) [XH] = 0.30 M, and (d) XH/CH_3CN (1/1). Reprinted with permission from ref[28]. Copyright © 1997, American Chemical Society.

Although O_2 does not react with wO, it does react all species derived from interaction between wO and an organic substrate, so that the yield of O_2 consumption can be equated to the yield of formation radicals formed from wO. A small consumption of O_2 was also found in pure acetonitrile, which maintained its reaction with wO, although under normal conditions it's preferred to consider acetonitrile an inert substrate. With the addition of propanol, the consumption of O_2 increased sharply.

When oxygen is not present, wO decays and forms a species that has one less electron, as oxygen prevents the formation of the one-electron-reduced

species, $W_{10}O_{32}^{5-}$ reacts with oxygen to produce a peroxy species. Irradiation in the presence of both propan-2-ol and O_2 results in the formation of acetone and hydrogen peroxide, which can further decay under reaction conditions.

The reaction between wO and alcoholic substrates involves hydrogen-atom abstraction. It has been observed that propan-2-ol reacts faster than acetonitrile, suggesting a hydrogen atom abstraction mechanism. Light-induced hydrogen-atom abstraction are consistent as well[28].

Other solvents such as acetone or methanol were also investigated. The degradation of wO in various alcohols and acetone was studied after excitation by a 15 ns laser pulse (Figure 1.9.7). For acetone, the decay profile of wO at 780 nm turned out to be similar to the profile for acetonitrile: in acetone, wO has a lifetime of 62 ± 5 ns, which is almost identical to the value in acetonitrile, but the yield of one-electron-reduced species was higher in acetone, which showed its greater reactivity towards wO[41].

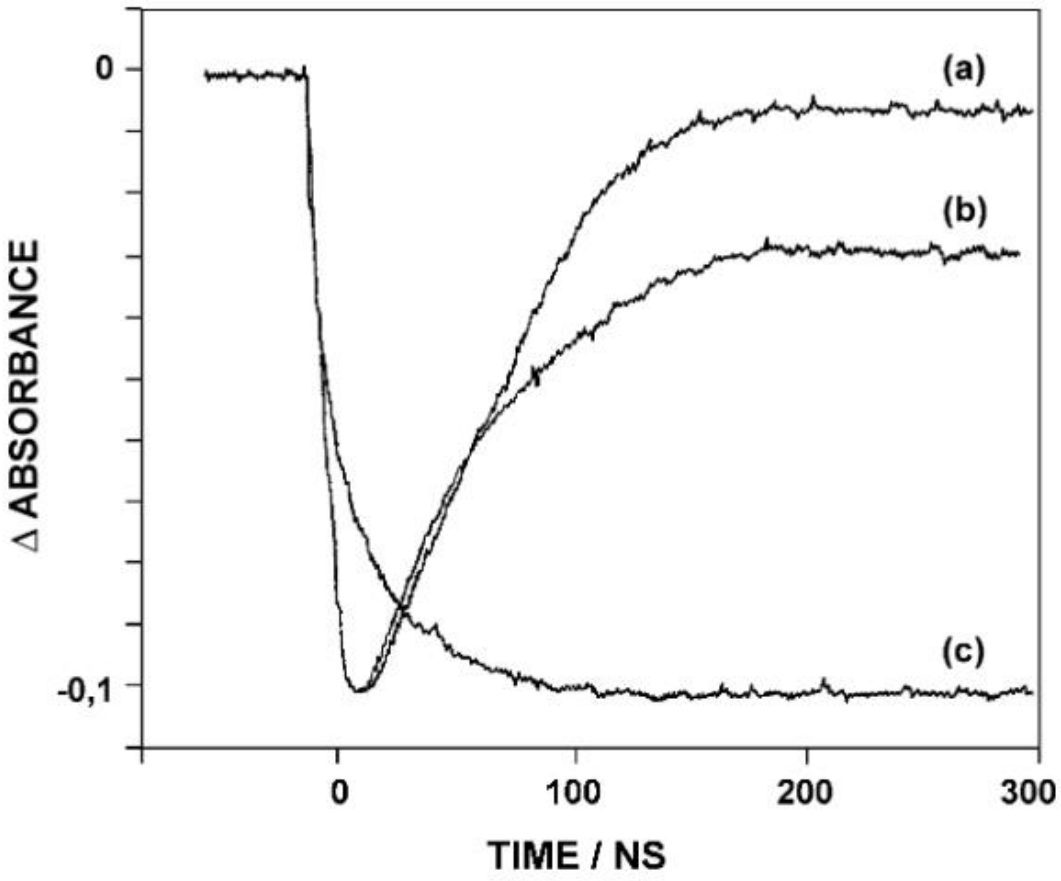

Figure 1.9.7: Kinetic profiles, normalized to the initial absorbance, observed at 780 nm showing decay of wO as generated following 355 nm excitation with a 15 ns laser pulse of 1.1×10^{-4} M sodium decatungstate air-saturated acetonitrile (a), acetone (b), and methanol (c) solutions. Reprinted with permission from ref[41].Copyright © 2006 Elsevier.

DT appears to exhibit especially interesting properties as a photocatalyst. Tetrabutylammonium decatungstate (TBADT), which has a high photocatalytic activity, has found widespread application in synthetic reactions involving the C–H bond activation in organic molecules such as alcohols[42], aldehydes, or alkanes[29,31,35].

In photocatalytic C-H bond functionalization processes promoted by DT, the rate of hydrogen abstraction (k_r) is greatly influenced by two factors: the

polarity of the C-H bond in the transition state and the level of steric hindrance. The excited DT species is highly electrophilic, which leads to a certain degree of selectivity in the hydrogen abstraction process. Specifically, DT tends to abstract more hydridic and sterically accessible C-H bonds preferentially[29,35].

Dondi et al. have demonstrated that TBADT photocatalysis is viable and a rather general method for the mild functionalization of aliphatic C-H bonds. Their results also suggest that, besides oxygenation, TBADT photocatalysis offers the added benefit of being a convenient method for forming C-C bonds[43].

Reactivity of wO is usually explained by diffusion-controlled dynamic quenching and static quenching processes. When quenched with alkanes ($k \sim 10^6$-10^7 $M^{-1}s^{-1}$)[40,44,45], hydroperoxides are formed in a quantitative manner through the hydrogen-atom abstraction from wO followed by reaction with oxygen. Alkenes, on the other hand, can react through both hydrogen-atom-transfer at the allylic position of alkene to form the allyl radical, while electron transfer would lead to oxidation of the double bond, yielding the cation radical product. It was also shown that the reaction of wO with alkenes leads to the formation of longer-lived complexes[40]. For cycloalkanes quenching rate constants were measured between 10^7 and 10^8 $M^{-1}s^{-1}$with increase with the ring size increasing[44]. As a stronger oxidant, TBADT has a broader photocatalytic scope, enabling activation of alkanes and their simple derivatives.

1.10 References

1. Rohatgi-Mukherjee KK. *Fundamentals of Photochemistry*. New Age International; 1978. Accessed March 29, 2024.
2. Lakowicz JR. Introduction to Fluorescence. In: *Principles of Fluorescence Spectroscopy*. Springer US; 1999:1-23.
3. Capaldo L, Ravelli D. Hydrogen Atom Transfer (HAT): A Versatile Strategy for Substrate Activation in Photocatalyzed Organic Synthesis. *Eur J Org. Chem*. 2017;2017(15):2056-2071.
4. Laudadio G, Deng Y, Van Der Wal K, et al. C(sp^3)–H functionalizations of light hydrocarbons using decatungstate photocatalysis in flow. *Science*. 2020;369(6499):92-96.
5. Angioni S, Ravelli D, Emma D, Dondi D, Fagnoni M, Albini A. Tetrabutylammonium Decatungstate (Chemo)selective Photocatalyzed, Radical C-H Functionalization in Amides. *Adv Synth Catal*. 2008;350(14-15):2209-2214.
6. Perry IB, Brewer TF, Sarver PJ, Schultz DM, DiRocco DA, MacMillan DW. Direct arylation of strong aliphatic C–H bonds. *Nature*. 2018;560(7716):70-75.
7. Esposti S, Dondi D, Fagnoni M, Albini A. Acylation of electrophilic olefins through decatungstate-photocatalyzed activation of aldehydes. *Angew Chem-Int Ed Engl-*. 2007;46(14):2531.
8. Capaldo L, Fagnoni M, Ravelli D. Vinylpyridines as Building Blocks for the Photocatalyzed Synthesis of Alkylpyridines. *Chem – Eur J*. 2017;23(27):6527-6530.

9. Fan P, Zhang C, Zhang L, Wang C. Acylation of Aryl Halides and α-Bromo Acetates with Aldehydes Enabled by Nickel/TBADT Cocatalysis. *Org Lett*. 2020;22(10):3875-3878.

10. Ravelli D, Protti S, Fagnoni M. Decatungstate Anion for Photocatalyzed "Window Ledge" Reactions. *Acc Chem Res*. 2016;49(10):2232-2242.

11. Ryu I, Tani A, Fukuyama T, Ravelli D, Montanaro S, Fagnoni M. Efficient C–H/C–N and C–H/C–CO–N Conversion via Decatungstate-Photoinduced Alkylation of Diisopropyl Azodicarboxylate. *Org. Lett*. 2013;15(10):2554-2557.

12. Capaldo L, Wan T, Noël T, et al. Decatungstate-Mediated C (sp^3)–H Heteroarylation via Radical-Polar Crossover in Batch and Flow. Published online 2023. Accessed May 12, 2024.

13. Wang X, Dong J, Liu Y, Song H, Wang Q. Decatungstate as a direct hydrogen atom transfer photocatalyst for synthesis of trifluromethylthioesters from aldehydes. *Chin Chem Lett*. 2021;32(10):3027-3030.

14. Dong J, Wang X, Wang Z, Song H, Liu Y, Wang Q. Formyl-selective deuteration of aldehydes with D_2O via synergistic organic and photoredox catalysis. *Chem Sci*. 2020;11(4):1026-1031.

15. Halperin SD, Fan H, Chang S, Martin RE, Britton R. A Convenient Photocatalytic Fluorination of Unactivated C-H Bonds. *Angew Chem*. 2014;126(18):4778-4781.

16. Halperin SD, Kwon D, Holmes M, et al. Development of a Direct Photocatalytic C–H Fluorination for the Preparative Synthesis of Odanacatib. *Org Lett*. 2015;17(21):5200-5203.

17. Yuan Z, Britton R. Development and application of decatungstate catalyzed C–H 18 F- and 19 F-fluorination, fluoroalkylation and beyond. *Chem Sci*. 2023;14(45):12883-12897.
18. West JG, Huang D, Sorensen EJ. Acceptorless dehydrogenation of small molecules through cooperative base metal catalysis. *Nat Commun*. 2015;6(1):10093.
19. Hill CL. Introduction of Functionality into Unactivated Carbon-Hydrogen Bonds. Catalytic Generation and Nonconventional Utilization of Organic Radicals. *Synlett*. 1995;1995(02):127-132.
20. Scaiano JC. Nanosecond Laser Flash Photolysis: A Tool for Physical Organic Chemistry. In: *Reactive Intermediate Chemistry*. John Wiley & Sons, Ltd; 2003:847-871.
21. Granite. Flash Photolysis | An Introduction using the LP980 Spectrometer. Edinburgh Instruments. Accessed July 25, 2024.
22. Yang Z, Li J, Niu J, Wang J. Polyoxotantalate chemistry: from synthetic strategies to structural diversity and applications. *Dalton Trans*. 2023;52(15):4632-4642.
23. Ammam M. Polyoxometalates: formation, structures, principal properties, main deposition methods and application in sensing. *J Mater Chem A*. 2013;1(21):6291-6312.
24. Chapter 1 Introduction to Polyoxometalates andScope of the Work. Accessed April 7, 2024. https://www.tdx.cat/bitstream/handle/10803/9069/capitol1.pdf?sequence=2
25. Tanielian C. Decatungstate photocatalysis. *Coord Chem Rev*. 1998;178-180:1165-1181.

26. Duncan DC, Netzel TL, Hill CL. Early-Time Dynamics and Reactivity of Polyoxometalate Excited States. Identification of a Short-Lived LMCT Excited State and a Reactive Long-Lived Charge-Transfer Intermediate following Picosecond Flash Excitation of [W10O32]4- in Acetonitrile. *Inorg Chem*. 1995;34(18):4640-4646.

27. Yamase T, Usami T. Photocatalytic dimerization of olefins by decatungstate (VI),$[W_{10}O_{32}]^{4-}$, in acetonitrile and magnetic resonance studies of photoreduced species. *J Chem Soc Dalton Trans*. 1988;(1):183-190.

28. Tanielian C, Duffy K, Jones A. Kinetic and Mechanistic Aspects of Photocatalysis by Polyoxotungstates: A Laser Flash Photolysis, Pulse Radiolysis, and Continuous Photolysis Study. *J Phys Chem B.* 1997;101(21):4276-4282.

29. Waele VD, Poizat O, Fagnoni M, Bagno A, Ravelli D. Unraveling the Key Features of the Reactive State of Decatungstate Anion in Hydrogen Atom Transfer (HAT) Photocatalysis. *ACS Catal*. 2016;6(10):7174-7182.

30. Singh PP, Sinha S, Gahtori P, Tivari S, Srivastava V. Recent advances of decatungstate photocatalyst in HAT process. *Org Biomol Chem*. Published online 2024. Accessed March 29, 2024.

31. Ravelli D, Fagnoni M, Fukuyama T, Nishikawa T, Ryu I. Site-Selective C–H Functionalization by Decatungstate Anion Photocatalysis: Synergistic Control by Polar and Steric Effects Expands the Reaction Scope. *ACS Catal*. 2018;8(1):701-713.

32. Texier I, Delaire JA, Giannotti C. Reactivity of the charge transfer excited state of sodium decatungstate at the nanosecond time scale. *Phys Chem Chem Phys*. 2000;2(6):1205-1212.

33. Capaldo L, Ravelli D, Fagnoni M. Direct Photocatalyzed Hydrogen Atom Transfer (HAT) for Aliphatic C–H Bonds Elaboration. *Chem Rev*. 2022;122(2):1875-1924.

34. Suzuki K, Mizuno N, Yamaguchi K. Polyoxometalate Photocatalysis for Liquid-Phase Selective Organic Functional Group Transformations. *ACS Catal*. 2018;8(11):10809-10825.

35. Tzirakis MD, Lykakis IN, Orfanopoulos M. Decatungstate as an efficient photocatalyst in organic chemistry. *Chem Soc Rev*. 2009;38(9):2609-2621.

36. Ermolenko LP, Delaire JA, Giannotti C. Laser flash photolysis study of the mechanism of photooxidation of alkanes catalysed by decatungstate anion. *J Chem Soc Perkin Trans 2*. 1997;(1):25-30.

37. Yamase T, Takabayashi N, Kaji M. Solution photochemistry of tetrakis (tetrabutylammonium) decatungstate (VI) and catalytic hydrogen evolution from alcohols. *J Chem Soc Dalton Trans*. 1984;(5):793-799.

38. Duncan DC, Hill CL. Synthesis and Characterization of the Mixed-Valence Diamagnetic Two-Electron-Reduced Isopolytungstate,$[W_{10}O_{32}]^{6-}$. Evidence for an Asymmetric d-Electron Distribution over the Tungsten Sites. *Inorg Chem*. 1996;35(20):5828-5835.

39. Kothe T, Martschke R, Fischer H. Photoreactions of the decatungstateanion $W_{10}O_{32}^{4-}$ with organic substrates in solution studied by EPR and kinetic absorption spectroscopy: an example for the persistent radical effect. *J Chem Soc Perkin Trans 2*. 1998;(3):503-508.

40. Tanielian C, Seghrouchni R, Schweitzer C. Decatungstate Photocatalyzed Electron-Transfer Reactions of Alkenes. Interception of the

Geminate Radical Ion Pair by Oxygen. *J Phys Chem A*. 2003;107(8):1102-1111.

41. Tanielian C, Cougnon F, Seghrouchni R. Acetone, a substrate and a new solvent in decatungstate photocatalysis. *J Mol Catal Chem*. 2007;262(1-2):164-169.

42. Guo ML. Quaternary ammonium decatungstate catalyst for oxidation of alcohols. *Green Chem*. 2004;6(6):271-273.

43. Dondi D, Fagnoni M, Albini A. Tetrabutylammonium Decatungstate-Photosensitized Alkylation of Electrophilic Alkenes: Convenient Functionalization of Aliphatic C-H Bonds. *Chem – Eur J*. 2006;12(15):4153-4163.

44. Duncan DC, Fox MA. Early Events in Decatungstate Photocatalyzed Oxidations: A Nanosecond Laser Transient Absorbance Reinvestigation. *J Phys Chem A*. 1998;102(24):4559-4567.

45. Duncan DC, Jaynes BS, Netzel TL, Hill CL. Dynamic behavior in the light and dark phases of alkane photochemical functionalization by $W_{10}O_{32}^{4-}$. *Proc Indian Acad Sci*. 1995;107(6):729-733.

Chapter 2: Materials and methods

2.1 Introduction

This chapter provides a detailed description of the experimental techniques and methods used during the study. The primary techniques employed were steady-state absorption and nano-second transient absorption techniques, i.e., laser flash photolysis. These techniques were usedunder different environmental conditions.

2.2 Instrumentation

2.2.1 Steady state absorption measurements

Depending on the type of experiments, the ground state electronic absorption spectra were recorded at room temperature on the Cary 50, Cary 100, Cary 60 coupled with optical fiber, or Cary 7000 spectrometer using a 1 cm path length quartz cuvette. The sample was compared to a background measured using a matched cuvette containing pure solvent in each measurement and the background was subtracted.

Instrument	**Mode**	**Spectral range (nm)**	**Light Source**
Cary 50	Single beam	190-800	Xenon flash lamp

Cary 100	Dual-beam	190-800	Tungsten halogen: Visible and Deuterium arc: UV
Cary 60 with Optical Fiber	Dual-beam	190-1100	Xenon flash lamp
Cary 7000	Dual-beam	175-3300	Tungsten halogen: Visible and Deuterium arc: UV

Table 2.2.1: Brief technical details of the used UV-Vis instruments

2.2.2 ns-Transient Absorption/Laser Flash Photolysis (LFP)

Laser photolysis is a technique in which a laser pulse causes the formation of transient species, such as a radical intermediate or a short-lived excited state, within a sample. Subsequent changes, as the sample returns to its original state or final product, are recorded over time. A laser photolysis spectrometer is capable of monitoring changes in absorbance over time by switching on a secondary light source (monitor beam) near the excitation pulse passing through the sample. This approach, also called transient absorption (TA), allows studies to be performed on various time scales, from picoseconds to seconds[1].

Application of complex transient absorption experiments spanning from nanoseconds to seconds, facilitating the identification of free radicals, triplet excited states and intermediates involved in charge transfer reactions. This technique plays a critical role in studying reaction kinetics and determining the lifetime of non-emissive triplet states, as well as in detecting elusive

intermediates in light-induced reactions. Consequently, it serves as an important tool in advancing basic research in photochemistry, materials science, and photobiology[2].

Our laboratory has a custom-built LFP setup controlled by Luzchem Research Inc. software. The schematic diagram of LFP is shown in Figure 2.2.2.1.

At our lab, for LFP experiments, nanosecond to millisecond time scales are performed with a Q-switched Nd:YAG laser (Continuum Surelite II -10) as a pump source. The laser operated in the frequency tripled mode at 355 nm (6 ns, 1 Hz) and the energy is kept between ~ 10-15 mJ per pulse. The transient absorption was monitored in transmission mode using white light (probe) from a 300W xenon CW lamp. Pump and probe beams are spatially overlapped to generate a transient signal.

Further, the transmitted probe beam is re-imaged at the entrance slit of the monochromator. The monochromatic light, also known as the transient signal, is collected by a photomultiplier tube (PMT) powered by a high voltage source. The PMT signal is subsequently corrected in real time through a compensation circuit to remove any DC offset before being sent to the oscilloscope. The oscilloscope then processes the signal by averaging it over a predetermined number of pulses.

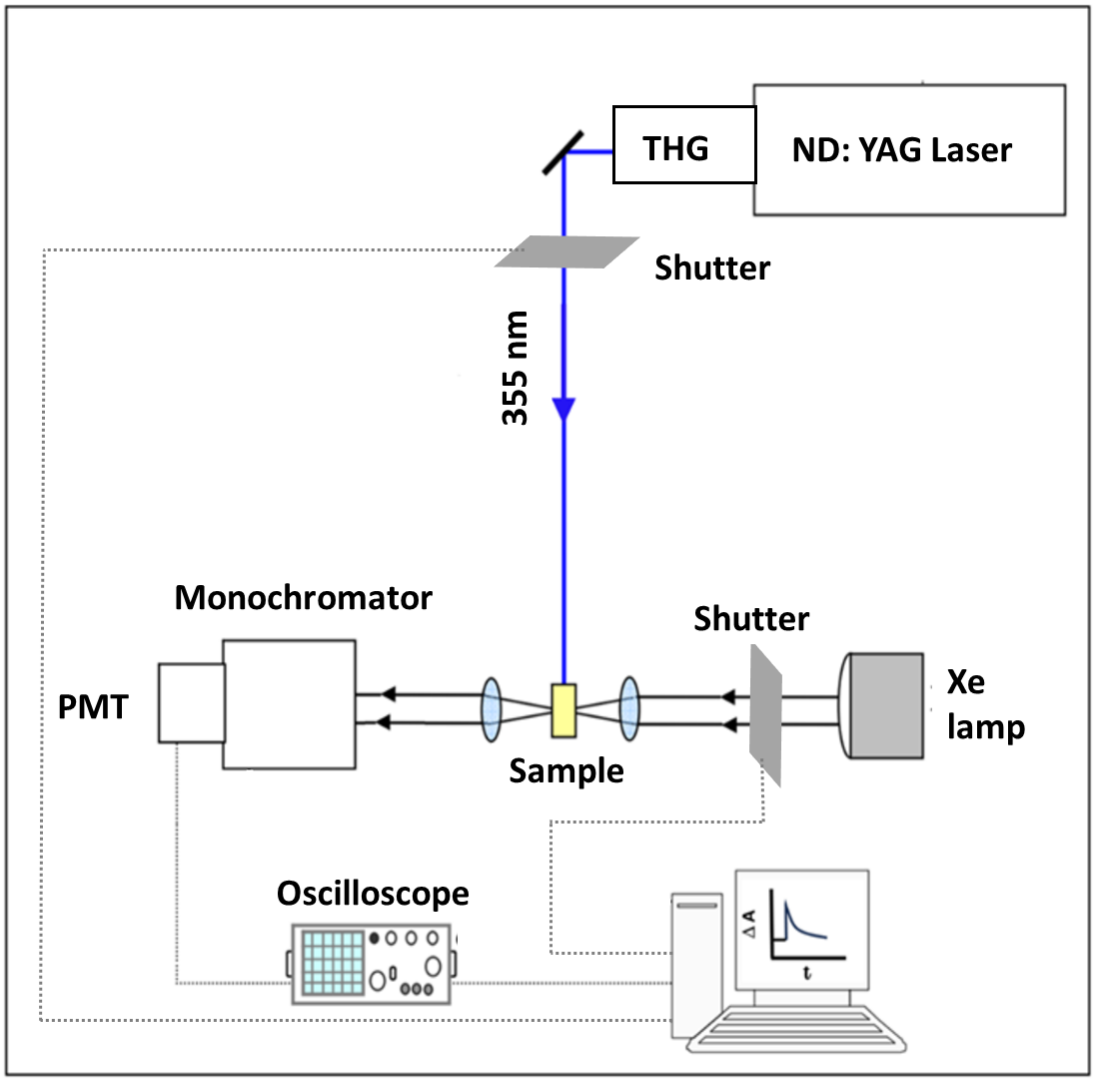

Figure 2.2.2.1: Schematic diagram of LFP setup. THG: Third harmonic generator.

Data were collected using Luzchem Inc. software. The kinetic profiles were obtained by collecting data at one particular wavelength and averaging over a determined number of shots. Transient UV-vis absorption spectra are acquired for a chosen kinetic curve of a particular time scale, usually every 10 nm in 280-800 nm spectral intervals.

The change in absorbance at time t is given by:

$$(Absorbancechange) = \Delta A = -log\frac{I_0}{I_t} = log\left(1 - \frac{signal}{I_0}\right) \quad (1)$$

Where I_0 and I_t are explained with the help of Figure 2.2.2.2. The laser fires at t=0 and causes an increase in absorbance in the sample. In Figure 2.2.2.2, the reference signal is acquired before laser excitation and leads to I_0[3].

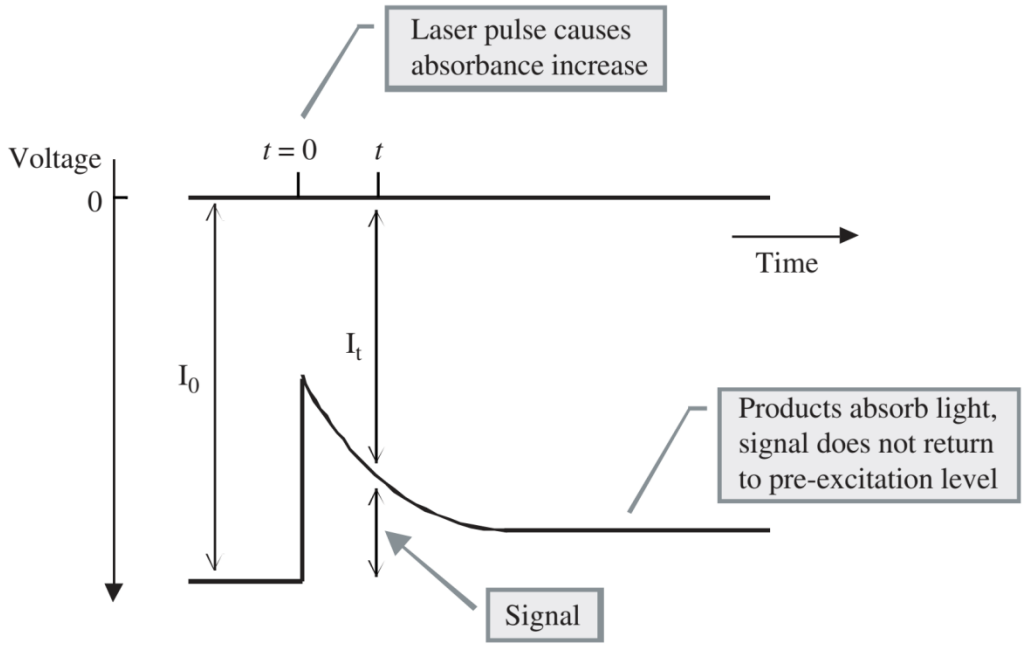

Figure 2.2.2.2: Time evolution of the photomultiplier output as an absorbing transient is generated and decays. Reproduced from ref[2] with permission. Copyright © 2004 John Wiley & Sons, Inc.

2.2.3 Singlet Oxygen and NIR measurements:

Singlet oxygen, referred to as an electronically excited form of molecular oxygen, is a less stable state compared to its ground electronic state. Its sensitization often involves the transfer of energy from a photocatalyst's excited state to the oxygen molecule (Figure 2.2.3.1). In singlet oxygen investigations, emission is usually detected around 1270 nm. These studies

pose challenges due to the significantly weaker emission of singlet oxygen in comparison to sensitizers[2].

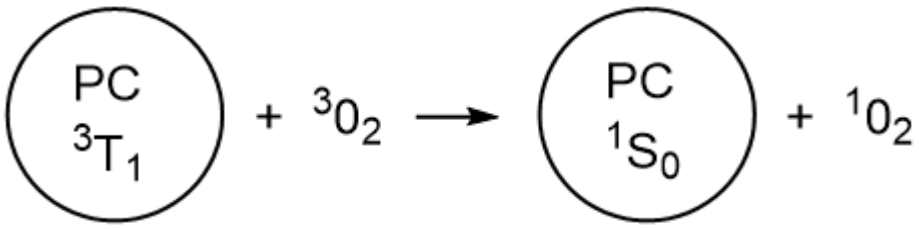

Figure 2.2.3.1: Mechanism of singlet oxygen production.

Singlet oxygen measurement is performed in our lab with a Q-switched Nd: YAG laser (Continuum Surelite II -10) as an excitation source. The laser operated in the frequency tripled mode at 355 nm (6 ns, 1Hz) and the energy is kept between ~ 10-15 mJ per pulse. The emission signal is monitored at the right angle to the excitation beam (Figure. 2.2.3).

Further, the emission signal is passed through the entrance slit of a monochromator. The monochromatic light (transient signal) is fed to a NIR photomultiplier tube (PMT) operating with a high-voltage supply. The PMT signal is subsequently corrected in real time through a compensation circuit to remove any DC offset before being sent to the oscilloscope. The oscilloscope then processes the signal by averaging it over a predetermined number of pulses. To prevent any damage to the NIR PMT from the residual of fundamental wavelength (1064 nm) of the Nd:Yag laser, a cut of filter (1150 nm) is placed in front of monochromator (not shown in Figure 2.2.3.2).

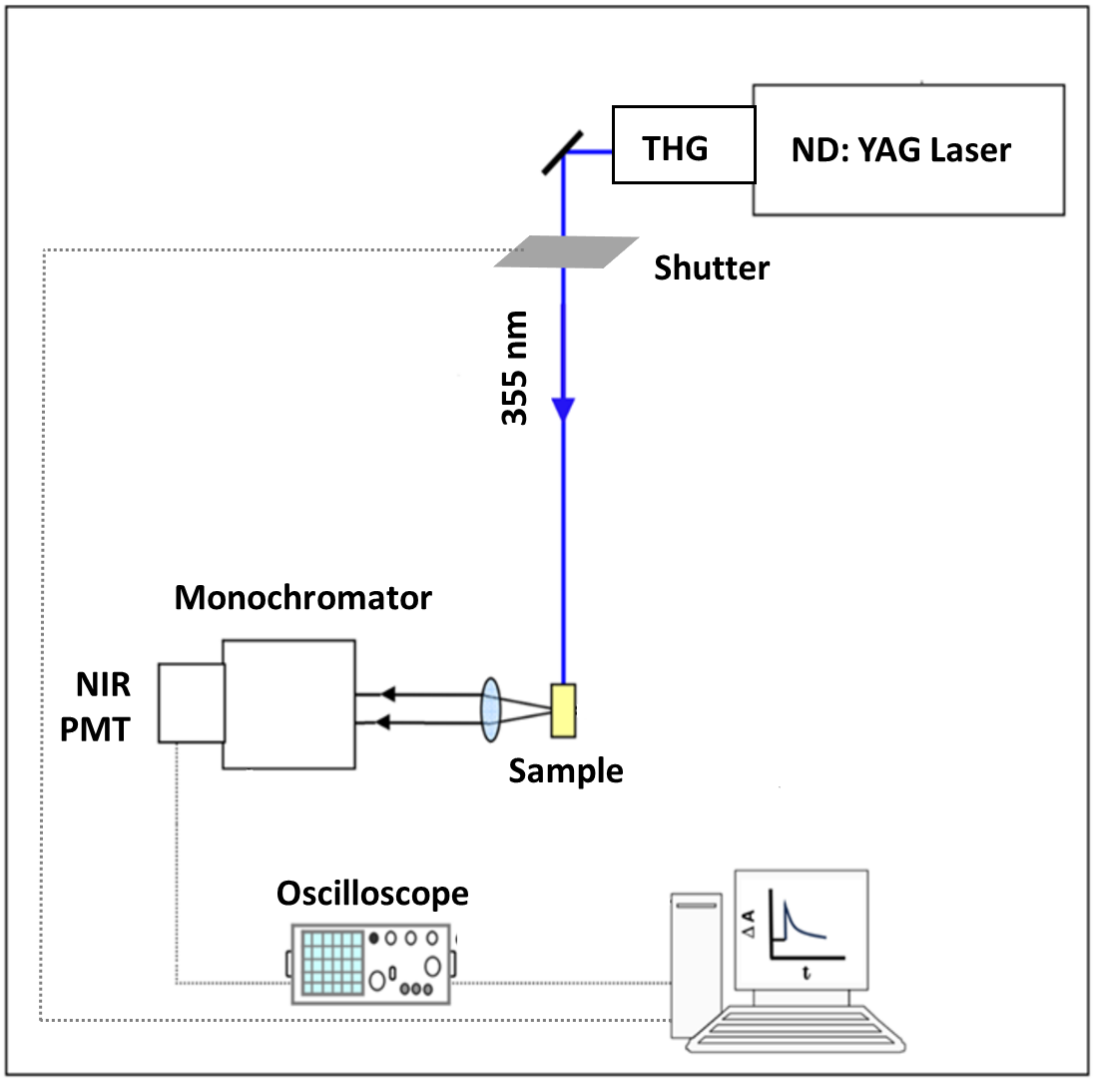

Figure 2.2.3.2: Schematic diagram of singlet oxygen measurement setup.

2.3 Reagents

Tetrabutylammonium decatungstate (TBADT) and other compounds were purchased from Sigma-Aldrich and used as received if not indicated otherwise. All solvents, cumene hydroperoxide, tert-Butyl hydroperoxide, hydrogen peroxide were bought from Fisher Chemicals. Sodiumdecatungstatewere synthesized by a procedure described below.

2.4 Sodium Decatungstate synthesis

The decatungstate was reported as versatile and inexpensive hydrogen atom transfer (HAT) catalyst[4]. This was intriguing as Sigma-Aldrich set high prices on decatungstate molecule. Looking further we discovered that decatungstate with different counter ions can be easily synthesized and the reagents are comparably cheap. There are few different methods of decatungstate synthesis reported[5–9].

Synthesis of $Na_4[W_{10}O_{32}]$: Sodium tungstate dihydrate (15 g, 45.5 mmol) was dissolved in deionized water (85 ml) and heated to 95 ^oC. Then a hot (95 °C) 1 M HCl solution was poured into a solution of sodium tungstate dihydrate and the reaction mixture was heated at 95 °C for 1 min. The yellowish solution was poured into a pre-cooled 1 L Erlenmeyer flask and left covered in an ice bath to cool for 10 min. After cooling the mixture to 10 ^oC, sodium chloride (60 g) was added. The mixture was kept in an ice bath for 1 hour and a white suspension formed. The suspension was filtered under vacuum through a large porous glass frit, the solid was washed with cold deionized water (20 ml), ethanol (20 ml) and diethyl ether (20 ml) and air dried for 30 min. Sodium decatungstate (7.51 g) was obtained[9].

2.5 Sample preparation

TBADT in ACN:1.6 mg of TBADT was dissolved in 10 ml of ACN; 3 ml of solution were transferred to the 1 cm cuvette with a syringe; The concentration was 0.05 mM. NIR emission measurements were taken at 1330 nm following 355 nm laser excitation.

TBADT in CD_3CN:1.6 mg of TBADT was dissolved in 10 ml of CD_3CN; 3 ml of solution were transferred to the 1 cm cuvette with a syringe; The concentration was 0.05 mM. NIR emission measurements were taken at 1330 nm following 355 nm laser excitation.

TBADT in 1:9 ACN/H_2O:1.6 mg of TBADT was dissolved in 9 ml of ACN mixed with 1 ml of milliQwater; 3 ml of solution were transferred to the 1 cm cuvette with a syringe; The concentration was 0.05 mM. NIR emission measurements were taken at 1330 nm following 355 nm laser excitation.

NaDT in 1:9 ACN/H_2O:4.8 mg of NaDT was dissolved in 9 ml of ACN mixed with 1 ml of milliQwater; 3 ml of solution were transferred to the 1 cm cuvette with a syringe; The concentration was 0.2 mM. NIR emission measurements were taken at 1330 nm following 355 nm laser excitation.

NaDT in 1:9 ACN/D_2O:4.8 mg of NaDT was dissolved in 9 ml of ACN mixed with 1 ml of deuterated water; 3 ml of solution were transferred to the 1 cm cuvette with a syringe; The concentration was 0.2 mM. NIR emission measurements were taken at 1330 nm following 355 nm laser excitation.

Quenching of TBADT by isopropanol (IPA):1.6 mg of TBADT was dissolved in 10 ml of ACN; 3 ml of solution were transferred to the 1 cm cuvette with a syringe. The concentration was 0.05 mM. IPA was injected with a syringe in the cuvette by portions to total concentration of 0.172, 0.339, 0.502, 0.662 M. NIR emission measurements were taken after each injection at 1330 nm following 355 nm laser excitation.

Quenching of TBADT by ethanol (EtOH):1.6 mg of TBADT was dissolved in 10 ml of ACN; 3 ml of solution were transferred to the 1 cm

cuvette with a syringe. The concentration was 0.05 mM.EtOH was injected with a syringe in the cuvette by portions to total concentration of 0.028, 0.057, 0.084, 0.112, 0.168, 0.225, 0.335, 0.552, 0.815 M. NIR emission measurements were taken after each injection at 1330 nm following 355 nm laser excitation.

Quenching of TBADT by methanol (MeOH):1.6 mg of TBADT was dissolved in 10 ml of ACN; 3 ml of solution were transferred to the 1 cm cuvette with a syringe. The concentration was 0.05 mM. MeOH was injected with a syringe in the cuvette by portions to total concentration of 0.325, 0.797, 1.170, 1.544 M. NIR emission measurements were taken after each injection at 1330 nm following 355 nm laser excitation.

Quenching of TBADT by triethylamine (TEA):1.6 mg of TBADT was dissolved in 10 ml of ACN; 3 ml of solution were transferred to the 1 cm cuvette with a syringe. The concentration was 0.05 mM. TEA was injected with a syringe in the cuvette by portions to total concentration of 0.00955, 0.019, 0.028, 0.038 M. NIR emission measurements were taken after each injection at 1330 nm following 355 nm laser excitation.

Quenching of TBADT by 1,4-cycloxehadiene:1.6 mg of TBADT was dissolved in 10 ml of ACN; 3 ml of solution were transferred to the 1 cm cuvette with a syringe. The concentration was 0.05 mM.1,4-Cycloxehadiene was injected with a syringe in the cuvette by portions to total concentration of 0.070, 0.170, 0.270, 0.470, 0.630 M. NIR emission measurements were taken after each injection at 1330 nm following 355 nm laser excitation.

Quenching of TBADT by triethylamine(TEA) and further protonation by trifluoroacetic acid (TFA):1.6 mg of TBADT was dissolved in 10 ml of ACN; 3 ml of solution were transferred to the 1 cm cuvette with a syringe. The concentration was 0.05 mM. TEA was injected with a syringe in the cuvette in concentration of 33 mM, after that trifluoroacetic acid was injected to the cuvette by portions to total concentration of 33, 50, 100 mM. NIR emission measurements were taken after each injection at 1330 nm following 355 nm laser excitation.

Quenching of Xanthone by tetrabutylammonium decatungstate (TBADT): Solution of Xanthone in ACN (OD= 0.5) was prepared, 3 ml of solution were transferred to 1 cm cuvette with a syringe and degassed under Ar for 30min. The solution of 1mM TBADT in ACN was injected with a syringe to the cuvette to the total concentration of 0.66, 1.3, 1.9, 3.2 mM; NIR emission measurements were taken after each injection at 610 nm following 355 nm laser excitation.

Quenching of Rose Bengal by tetrabutylammonium decatungstate (TBADT): Solution of Rose Bengal in ACN (OD= 0.45) was prepared, 3 ml of solution were transferred to 1 cm cuvette with a syringe and degassed under Ar for 30min. The solution of 1mM TBADT in ACN was injected with a syringe to the cuvette to the total concentration of 0.33, 0.66, 1.3, 1.6, 1.9, 2.3, 3.2 mM; NIR emission measurements were taken after each injection at 610 nm following 355 nm laser excitation.

Quenching of NaDT by cumene hydroperoxide: 1.6 mg of NaDT was dissolved in 10 ml of ACN; 3 ml of solution were transferred to the 1 cm cuvette with a syringe. The concentration was 0.05 mM. Cumene

hydroperoxide was injected with a syringe in the cuvette by portions to total concentration of 3.50, 7.10, 10.60, 14.00 mM. NIR emission measurements were taken after each injection at 1330 nm following 355 nm laser excitation.

Quenching of NaDT by tert-Butyl hydroperoxide: 1.6 mg of NaDT was dissolved in 10 ml of ACN; 3 ml of solution were transferred to the 1 cm cuvette with a syringe. The concentration was 0.05 mM. Tert-Butyl hydroperoxide was injected with a syringe in the cuvette by portions to total concentration of 47.00, 95.00, 141.00, 232.00 mM. NIR emission measurements were taken after each injection at 1330 nm following 355 nm laser excitation.

Quenching of NaDT by hydrogen peroxide:1.6 mg of NaDT was dissolved in 10 ml of ACN; 3 ml of solution were transferred to the 1 cm cuvette with a syringe. The concentration was 0.05 mM. Hydrogen peroxide was injected with a syringe in the cuvette by portions to total concentration of 108.00, 214.70, 343.00, 423.00 mM. NIR emission measurements were taken after each injection at 1330 nm following 355 nm laser excitation.

2.6 References

1. Granite. Flash Photolysis | An Introduction using the LP980 Spectrometer. Edinburgh Instruments. Accessed July 25, 2024.
2. Scaiano JT. *Photochemistry Essentials*. Vol 25. American Chemical Society; 2022. Accessed March 29, 2024.
3. Scaiano JC. Nanosecond Laser Flash Photolysis: A Tool for Physical Organic Chemistry. In: *Reactive Intermediate Chemistry*. John Wiley & Sons, Ltd; 2003:847-871.
4. Laudadio G, Govaerts S, Wang Y, et al. Selective C(sp^3)−H Aerobic Oxidation Enabled by Decatungstate Photocatalysis in Flow. *Angew Chem*. 2018;130(15):4142-4146.
5. Guo Y, Hu C, Wang X, et al. Microporous Decatungstates: Synthesis and Photochemical Behavior. *Chem Mater*. 2001;13(11):4058-4064.
6. Chemseddine A, Sanchez C, Livage J, Launay JP, Fournier M. Electrochemical and photochemical reduction of decatungstate: a reinvestigation. *Inorg Chem*. 1984;23(17):2609-2613.
7. Duncan DC, Netzel TL, Hill CL. Early-Time Dynamics and Reactivity of Polyoxometalate Excited States. Identification of a Short-Lived LMCT Excited State and a Reactive Long-Lived Charge-Transfer Intermediate following Picosecond Flash Excitation of $[W_{10}O_{32}]^{4-}$ in Acetonitrile. *Inorg Chem*. 1995;34(18):4640-4646.
8. Li H, Jiang X, Zhu W, Lu J, Shu H, Yan Y. Deep Oxidative Desulfurization of Fuel Oils Catalyzed by Decatungstatesin the Ionic Liquid of [Bmim]PF_6. *Ind Eng Chem Res*. 2009;48(19):9034-9039.

9. Sarver PJ, Bacauanu V, Schultz DM, et al. The merger of decatungstate and copper catalysis to enable aliphatic C (sp^3)–H trifluoromethylation. *Nat Chem*. 2020;12(5):459-467.

Chapter 3: Characterization of triplet decatungstate behavior and its kinetics using NIR phosphorescence

3.1 Review

The photochemistry of decatungstate is a subject of interest due to its electron and hydrogen transfer reactions creating free radicals. These free radicals are used for many organic syntheses, including photoredox catalysis[1], gas-phase reactions[2], "window ledge" chemistry[3]. Decatungstate can be excited by laser flash photolysis creating short lived intermediates with reported lifetimes 50-100 ns depending on solvent used[4].

The mechanism of decatungstate transformation after being excited by a laser pulse was reported by Tanielian in 1998[5]. After excitation decatungstate anion $W_{10}O_{32}^{4-}$ turns into a very short lived charge-transfer excited state of decatungstate $W_{10}O_{32}^{4-*}$, which transforms to intermediate wO[3,6–8]. This intermediate can react with different substrates by hydrogen-transfer or electron-transfer mechanisms.

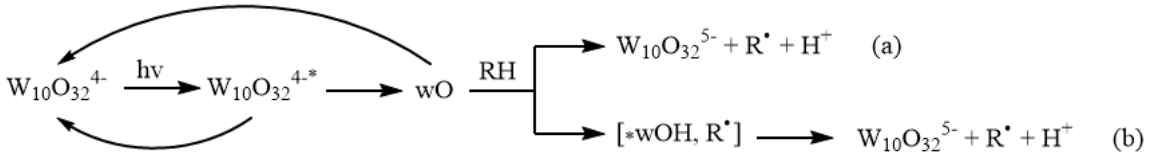

Figure 3.1.1: The mechanism of creating wO and it's reaction with substrates RH by electron-transfer (a) and hydrogen-transfer (b) mechanisms,ref[5]

The intermediate wO is quite similar in reactivity with triplets of ketones and alkoxyl radicals. It was reported that after excitation this intermediate

can abstract hydrogen atoms from different substrates such as alcohols[6,9,10], amines[4,9], hydrocarbons[9,11] and ethers[12].

In the presence of alcohols as a substrate the quantum yields of formation of radicals were measured by the consumption of O_2, as the wO itself does not react with oxygen. The yields for propan-2-ol, butan-1-ol and 2-methylpropan-2-ol for 0.1M f substrate in 0.55mM sodium decatungstate were 0.065, 0.23 and 0.05, respectively[5].

In the presence of amines the decay of DT signal was also observed. The quantum yield was calculated using the intermediate wO transient absorbance as an internal actinometer standard at 780 nm. Texier and others used the wO transient as a reference to determine the quantum yield of the reduced form of decatungstate. They reported the quantum yields for phenylamine, diphenylamine, triphenylamine, triethylamine, diethylamine and ethylamine[4].

Oxidative reaction with hydrocarbons could occur by a mechanism that involves the interaction of an excited state of sensitizer with the substrate, creating active radicals. These radicals react with oxygen, regenerating the sensitizer and forming peroxyl radicals or superoxide radicals. The quenching constants were reported: 1-hexene, trans-3-hexene, 2-methyl-2-pentene, 2,3-dimethylbutene, cyclohexene[11].

Intermediate wO was suggested to be triplet. There was no significant evidence to support this theory. Unlike most triplets, wO cannot be quenched by oxygen. This is probably the reason scientists were hesitant of calling wO the triplet.

In this chapter we will show that decatungstate intermediate wO actually is a triplet and why it does not make singlet oxygen. This work was done in collaboration with another member of our research group, Saba Didarataee, and with the support of Dr. Neeraj Joshi, and based on the published paper[13].

3.2 Results and discussion

We studied DT lifetime in acetonitrile (Figure3.2.1). There were some reports on DT lifetime was around 65-75 ns monitored by LFP at 780nm[4], but the quality of signals were poor, it had bad signal-to-noise ratios and were overlapping with the reduced form of decatungstate $DTH^{\bullet}$.

We were interested if the wO is DT triplet, so we can expect it to be quenched by oxygen and form singlet oxygen with a characteristic emission signal at 1270nm. In ACN, which we used as a solvent, it should live around 80μs[14].

When we irradiated the DT sample with a 355nm laser, we saw a broad emission signal with lifetime around 100 ns. This signal was the same whether the solution was under air, oxygen or argon. To ensure that our instrument was performing correctly, we performed a control experiment with Rose Bengal, which is a good sensitizer to make singlet oxygen ($^1O_2$). Just acetonitrile gave the instrument response function (IRF) signal (~25 ns, weak) as shown in Figure 3.2.1(A). An overlap of the two spectra ($^1O_2$ and ^{3}DT* emission) is shown in Figure 3.2.1(B). Notice that the long wavelength edge of the emission of NaDT is shifted about 60 nm with respect of the $^1O_2$ signal. The lifetime for decatungstate triplet(^{3}DT*) is around 800 times shorter than for $^1O_2$[15].

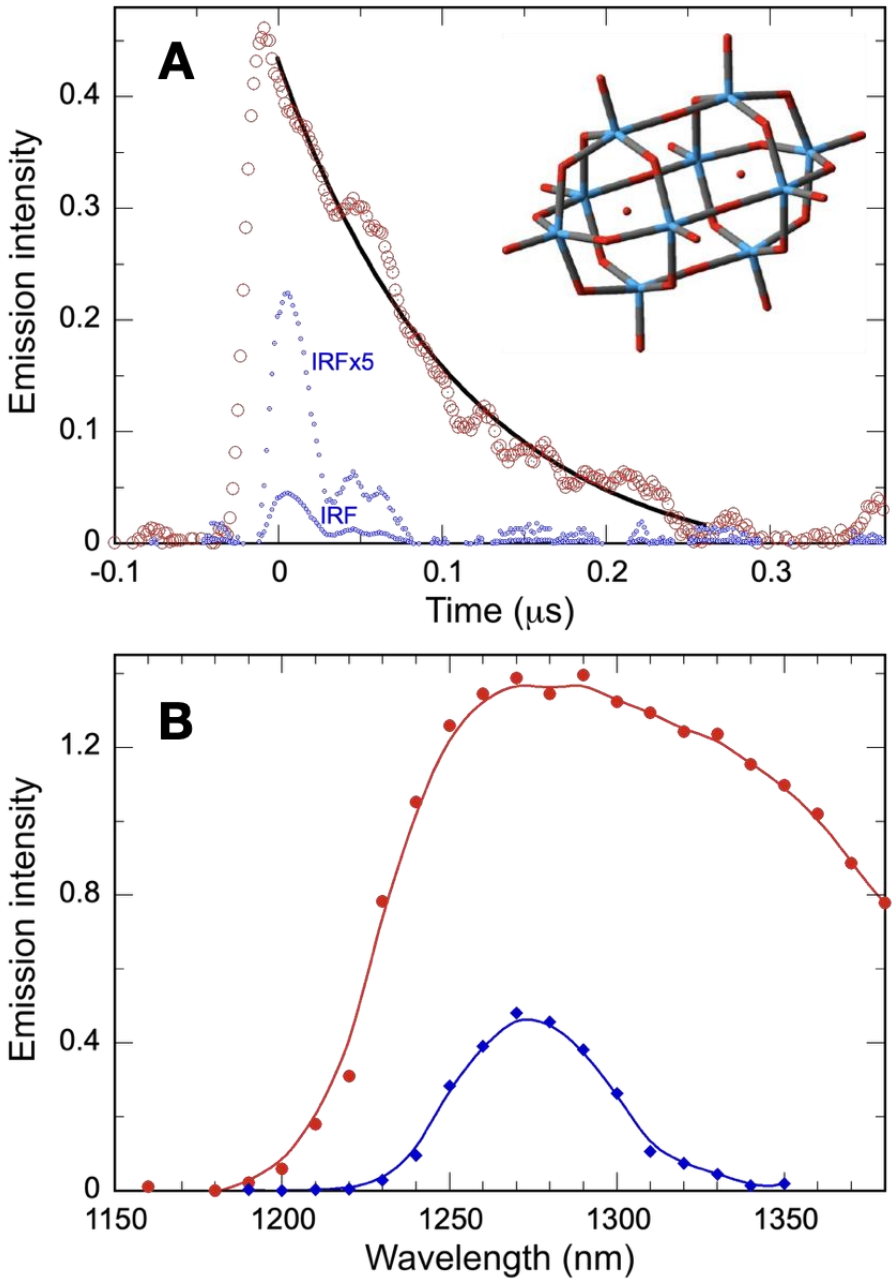

Figure 3.2.1: Decay of the TBADT phosphorescence monitored at 1330 nm in acetonitrile, along with the signal/noise recorded for acetonitrile alone, effectively an Instrument response function (IRF) which is far weaker than the emission observed for ^{3}DT*, and B:Emission spectra for ^{3}DT* (red) and singlet oxygen (blue) in acetonitrile; the former was sampled about 30 ns after the 355 nm laser pulse and the longer lived singlet oxygen about 2 μs after excitation, other parameters being identical. The singlet oxygen emission was sensitized by RB ($\mathbf{\Phi}_\Delta$=0.85). Reproduced from ref[13].

Singlet oxygen energy is around at 23 kcal/mol while the energy of the decatungstate triplet (Figure3.2.1(B)) is around 21kcal/mol. So ^{3}DT* just does not have enough energy to make singlet oxygen.

With the help of phosphorescence, ^{3}DT* can be easily studied using a reduced laser exposure. We measured lifetimes of sodium and tetrabutylammonium decatungstate under different conditions (Table 3.2.1).

DT	Concentration, mM	Solvent	Lifetime, ns
TBADT	0.05	CH_3CN	101
TBADT	0.05	1:9 CH_3CN:H_2O	43
NaDT	0.2	1:9 CH_3CN:H_2O	34
NaDT	0.2	1:9 CH_3CN:D_2O	80

Table 3.2.1: Lifetimes for ^{3}DT* in different solvents measured by NIR phosphorescence at 1330 nm.

The measured lifetime for TBADT in ACN was a little bit longer than for LFP because of bettersignal-to-noise ratio. NIR is a better tool to study decatungstate kineticks than LFP, as there is no offset which appears in LFP absorbance studies.

It is interesting to note that the triplet lifetimes for NaDT are 34 and 80 nanoseconds in 1:9 CH_3CN:H_2O and 1:9 CH_3CN:D_2O respectively, which

decays via firs-order kinetic, are showing a significant isotope effect (k_H/k_D = 2.4), as seen in (Figure 3.2.2). This is similar to the isotope effect observed for singlet oxygen, where the explanation involves an electronic to vibrational relaxation. This relaxation is enabled by a good matching of the excited state energy with C-H or O-H vibrations, predominantly the latter[16]. Recently, this explanation has been expanded by Ogilby and coworkers[17] to accommodate strong and weak coupling between the chromophore and the solvent molecules. We tentatively assign the observed behavior to weak coupling. However, a detailed analysis would require temperature-dependent studies in the solvents of interest. In contrast, for TBADT, the lifetimes in CH_3CN and CD_3CN are essentially the same, and any isotope effect is within our experimental error (Figure 3.2.3).

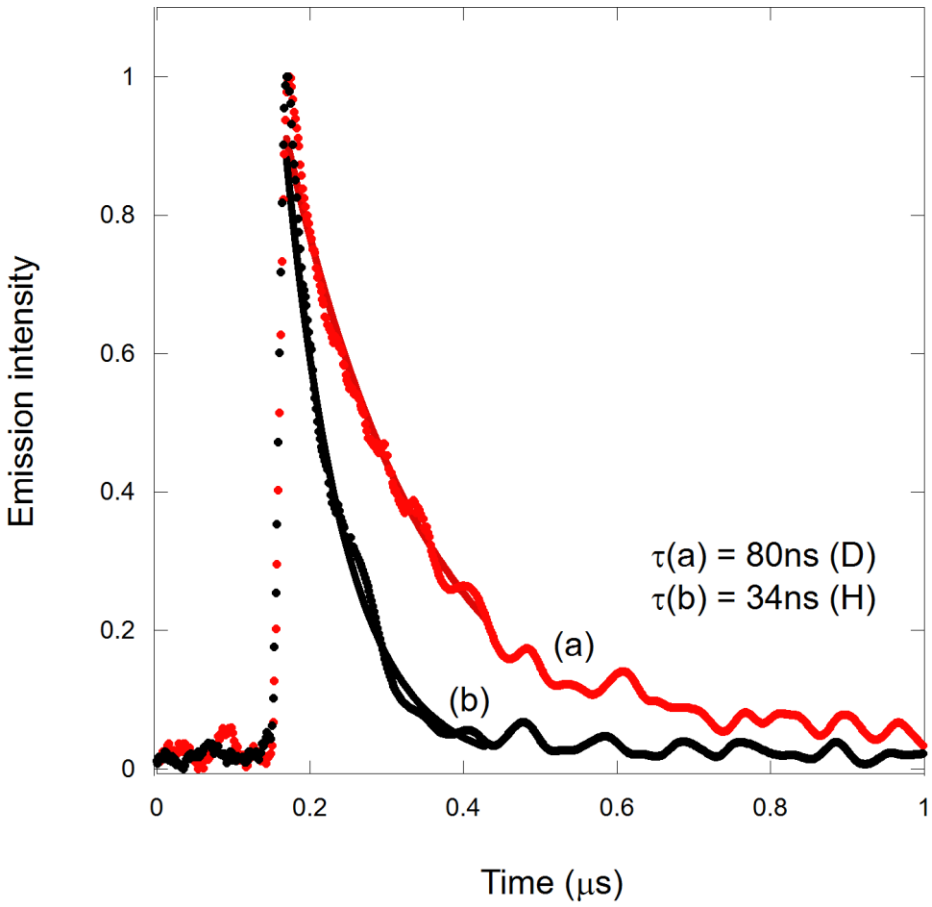

Figure 3.2.2: Emission from ^{3}DT* from NaDT in 1:9 $CH_3CN:H_2O$ (a) and in 1:9 $CH_3CN:D_2O$ (b).

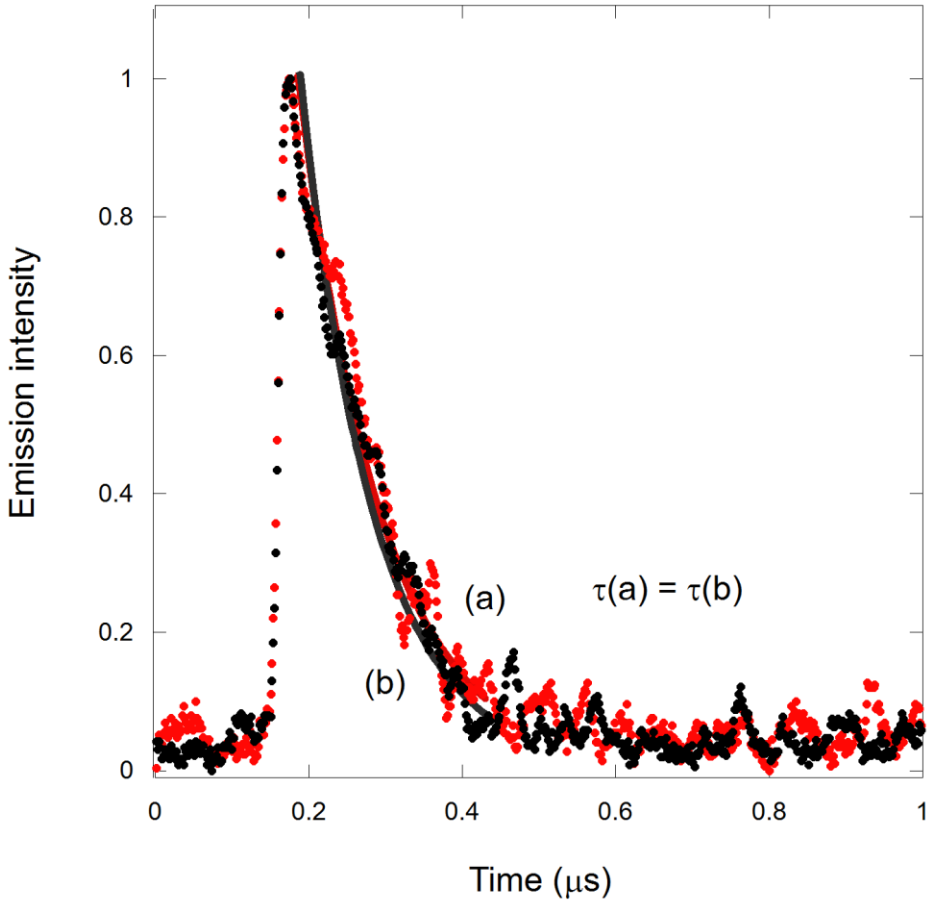

Figure 3.2.3: Emission from ^{3}DT* in CH_3CN (a) and CD_3CN (b).

For TBADT in CH_3CN/CD_3CN there were no significant difference and isotope effect was not observed. The difference was observed only for OH/OD case, even for singlet oxygen the effect of C-H/C-D bonds is weaker than for O-H/O-D ones[18,19].

We also studied the quenching of ^{3}DT* by five different hydrogen donors (Figure 3.2.4).

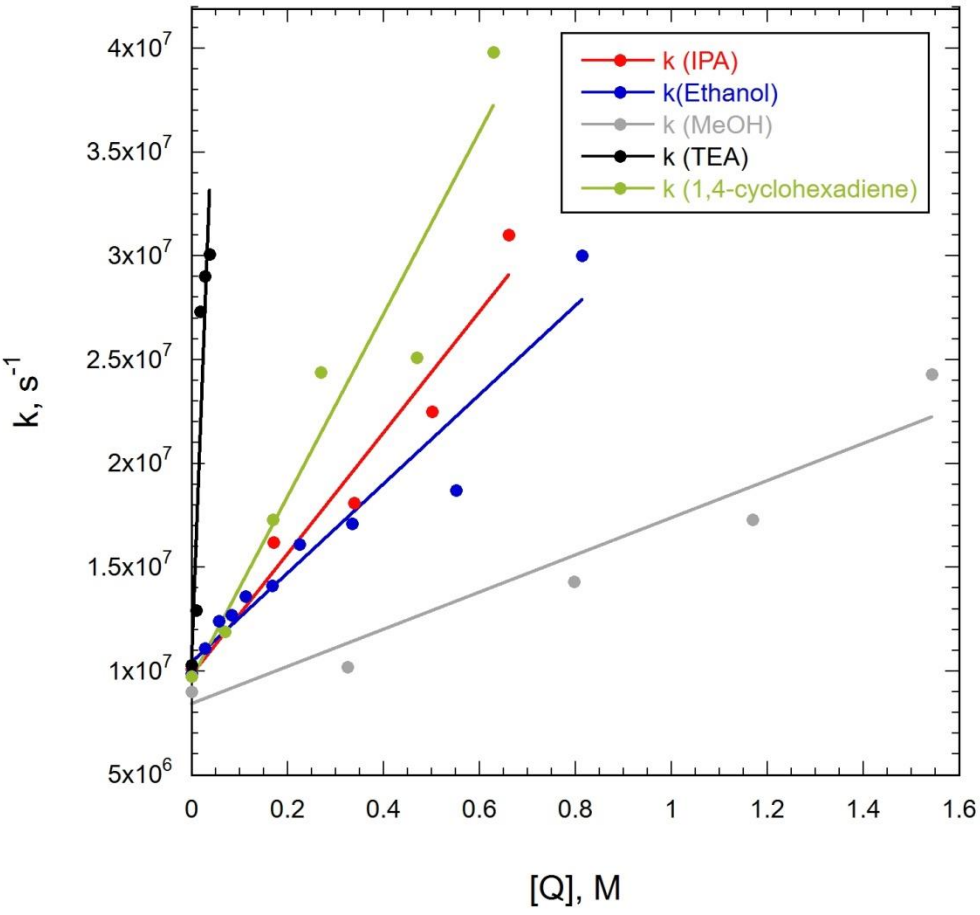

Figure 3.2.4: Quenching for TBADT in acetonitrile at room temperature for five quenchers: isopropanol (red), ethanol (blue), methanol (gray), triethylamine (black), 1,4-cyclohexadiene (green). Data are based on emission kinetics monitored at 1330 nm.

There are rate constants for many different quenchers reported in the literature; these are included in Table 3.2.2 along with our own measurements. The constants we got looked pretty comparative with those from the literature, they are at the same order of magnitude.

RH	DT	Solvent	k, 10^7 $M^{-1}s^{-1}$ (literature)	k, 10^7 $M^{-1}s^{-1}$ (this work)
2-butanol	NaDT	ACN	9.9[9] 19[4]	
2-propanol	TBADT	ACN	10[10]	2.9
2-propanol	NaDT	ACN	8.9[6]	
2-propanol	NaDT	acetone	4.9[6]	
methanol	NaDT	ACN	1.9[7]	
methanol	TBADT	ACN		0.9
ethanol	NaDT	ACN	520[4]	
ethanol	TBADT	ACN		2.1
Benzyl alcohol	NaDT	ACN	28[19]	
triethylamine	TBADT	ACN		60

triethylamine	NaDT	ACN	420[4]	
Diethyl aniline	NaDT	ACN	620[9]	
1-hexene	NaDT	ACN	4.2[11]	
cyclohexene	NaDT	ACN	11.9[11]	
cyclohexane	TBADT	ACN	4[10]	
cyclohexane	NaDT	ACN	3.25[9]	
cyclohexane	TBADT	ACN	4[10]	
cyclohexane-d_{12}	NaDT	ACN	1.09[9]	
cycloheptane	NaDT	ACN	5.6[9]	
1,4-cyclohexadiene	TBADT	ACN		30
Tetrahydrofuran	TBADT	ACN	23[20]	
$CH_3C\mathbf{H}(OH)Ph$	NaDT	ACN	14.4[19]	

Table 3.2.2: Constants for the reaction of ^{3}DT* with different hydrogen donors.

It is interesting that the quenching of DT by triethylamine can be reversed by the addition of trifluoroacetic acid. For [DT] = 0.05 mM, addition of 50 mM TFA returns the lifetime to the original unquenched value (Figure 3.2.5).

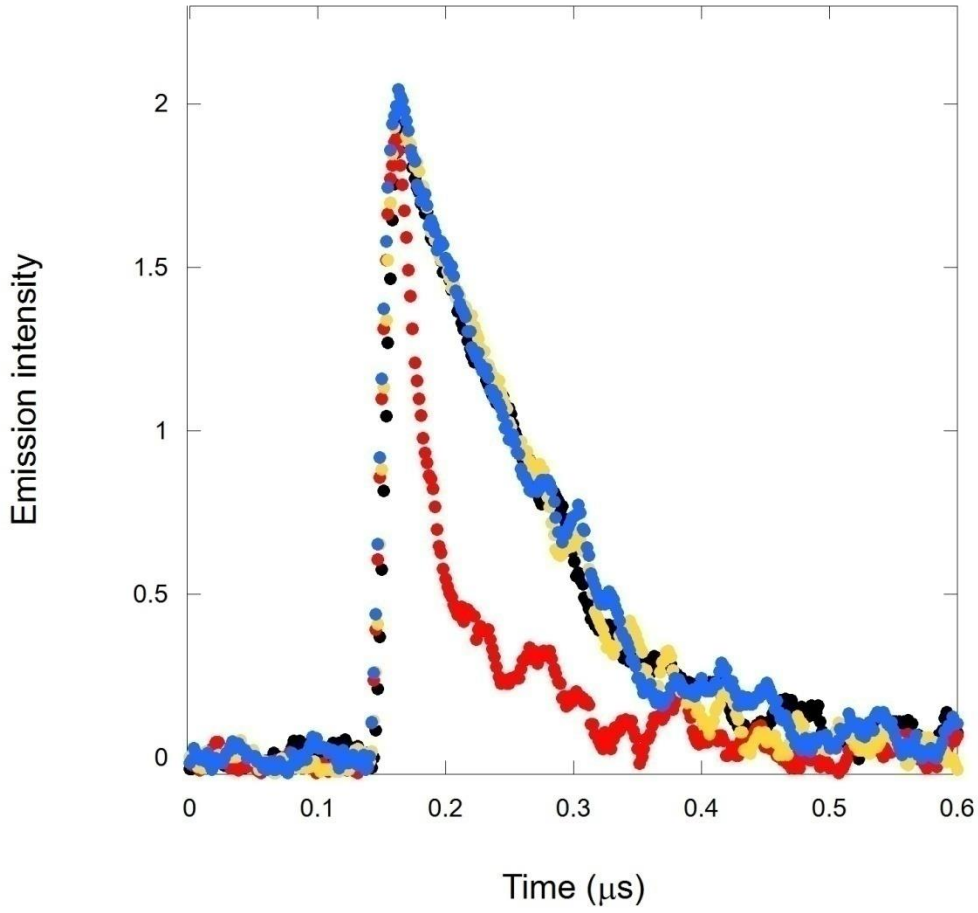

Figure 3.2.5: Quenching of TBADT triplet in acetonitrile with 33 mM triethylamine (TEA) with further addition of trifluoroacetic acid (TFA). Data was monitored at 1330 nm. The emission of ^{3}DT* is in black, with addition of 33 mM TEA (red), and further addition of 50 mM and 100 mM of TFA (yellow and blue respectively).

We were curious if ^{3}DT* can quench other triplets. For this we chose two molecules with high energy triplets: Xanthone (E_T ~ 74 kcal/mol)[21] and Rose Bengal (E_T ~ 41 kcal/mol)[22]. The Xanthone triplet quenching experiment had its own difficulties since the DT and Xanthone absorb light at the same laser wavelength at 355 nm (Figure 3.2.6).

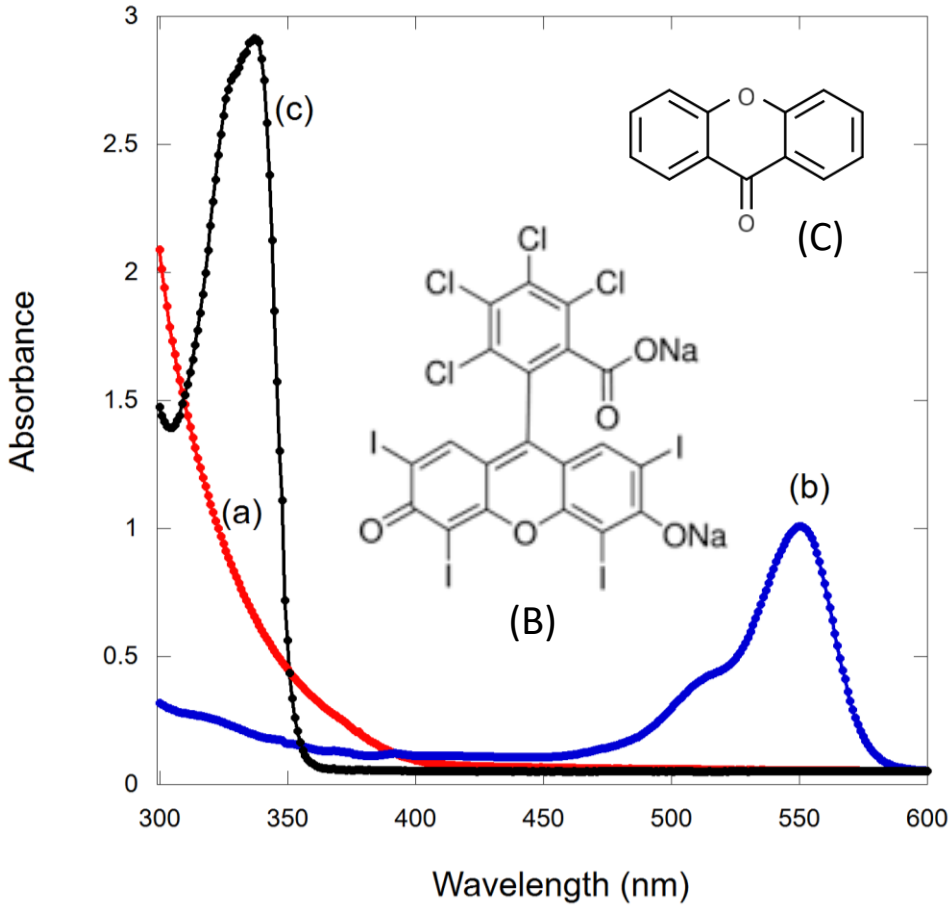

Figure 3.2.6: The comparison of absorption of DT (a), Rose Bengal (b), Xanthone (c) and the molecular structures of Rose Bengal (B) and Xanthone (C).

We had to use minimal amounts of DT to eliminate competitive absorption as much as possible. We obtained a rate constant of 9.3 x 10^9 $M^{-1}s^{-1}$ for Xanthone quenching by DT. We also observed the sensitized emission of

^{3}DT* in NIR region due to energy transfer between Xanthone and DT. However, this particular experiment cannot give very reliable results as DT also absorbs the 355nm wavelength (Figure 3.2.7).

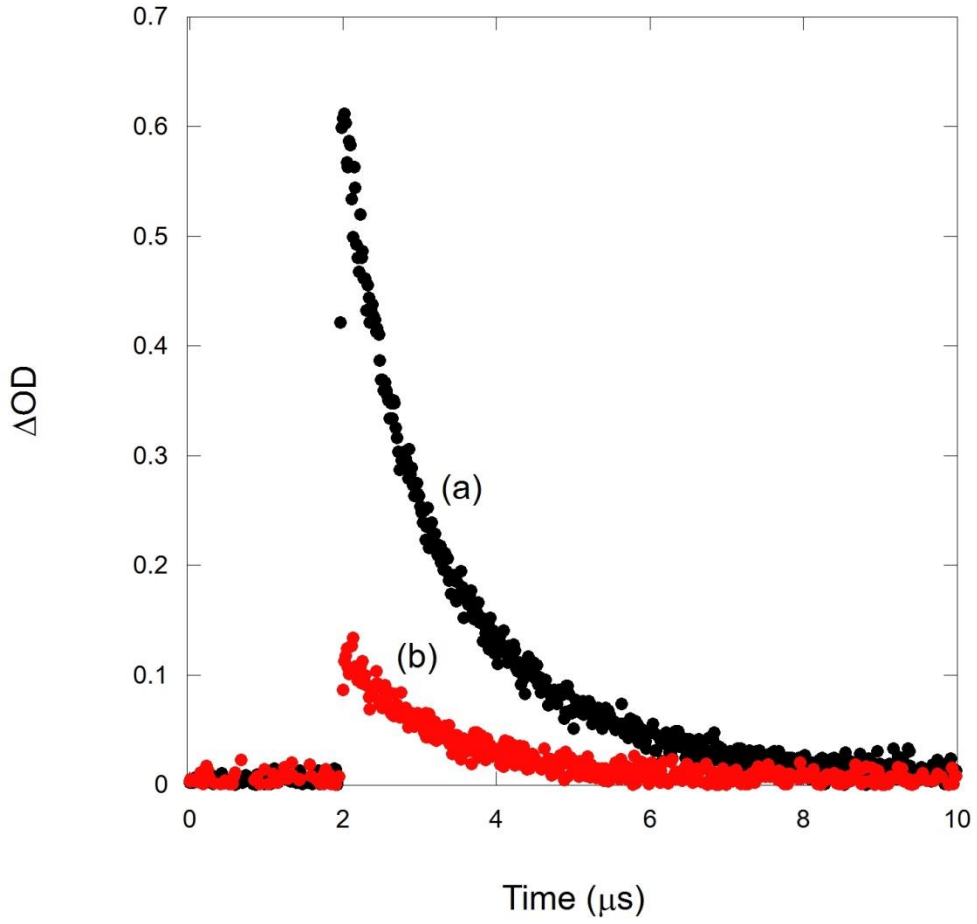

Figure 3.2.7: Decay of Xanthone triplet in absence (a) and presence (b) of 0.4mM DT, monitored at 610 nm.

We also performed similar experiments with Rose Bengal. This dye is well known as singlet oxygen sensitizer, so we performed this experiment under

argon with DT as a quencher. RB was excited by laser pulse at 532nm, which DT cannot absorb, thus we did not have a problem with competitive absorption(Figure 3.2.8). We obtained the rate constant 1.8×10^9 $M^{-1}s^{-1}$, although the lifetime of DT observed were longer than around 100ns (typical DT lifetime), because of the long lifetime of RB triplet, which continued to transfer energy to DT. The corresponding slopes for rate constants can be found in the appendix.

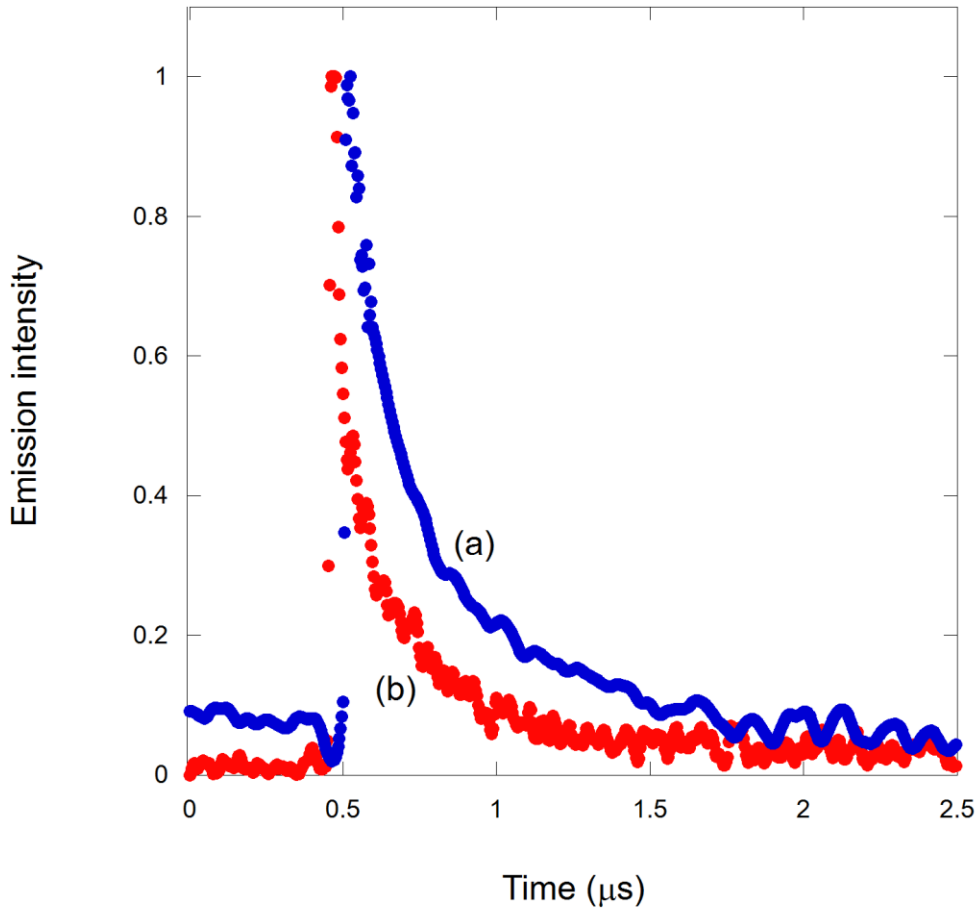

Figure 3.2.8: Decay of Rose Bengal triplet in the absence (a) and presence (b) of 0.4mM DT, monitored at 610 nm.

We also performed an experiment at low temperatures for NIR kinetics, using liquid nitrogen to refrigerate the sample. The lifetime at 77 K was 6.8 μs, which meant that even at this low temperature there is some reactivity. You can see some blue colour formed from DTH• (Figure 3.2. 9).

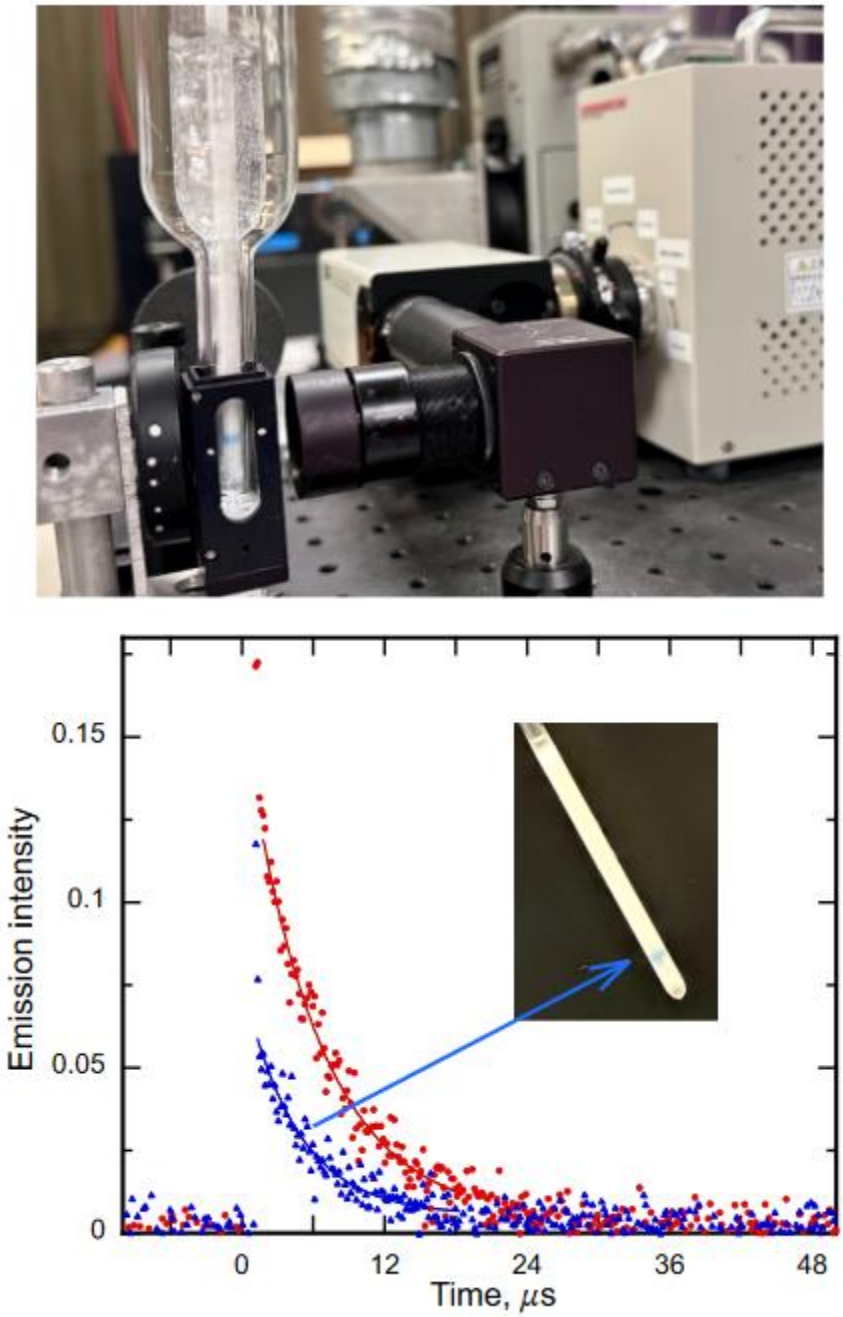

Figure 3.2.9: Top:Experimental low-temperature setup for NIR kinetics. Below: Decay kinetics at 77 K monitored at 1330 nm for a fresh sample (red) and for a sample exposed to ~200 laser pulses (blue) at 355 nm. Reproduced from ref[13].

3.3 Conclusions

In this chapter we showed that DT intermediate wO is actually a triplet, but it cannot be quenched by singlet oxygen because its energy is too low (21 kcal/mol). NIR data proves the triplet nature of wO. With a lifetime of 100 ns it is possible to study quenching by different substrates. In this chapter we showed five different substrates. The decay of the triplet state is facilitated by an electronic to vibrational conversion, which is particularly prominent in solvents containing O-H groups. This phenomenon is reminiscent of analogous processes observed in the case of singlet oxygen. By itself DT can act as a quencher, accepting energy from higher energy triplets such as Xanthone and Rose Bengal. The data presented, along with the discovery of NIR luminescence, represent powerful tools for discovering new catalytic pathways involving decatungstate.

3.4 References

1. Perry IB, Brewer TF, Sarver PJ, Schultz DM, DiRocco DA, MacMillan DW. Direct arylation of strong aliphatic C–H bonds. *Nature*. 2018;560(7716):70-75.

2. Laudadio G, Deng Y, Van Der Wal K, et al. C(sp^3)–H functionalizations of light hydrocarbons using decatungstate photocatalysis in flow. *Science*. 2020;369(6499):92-96.

3. Ravelli D, Protti S, Fagnoni M. Decatungstate Anion for Photocatalyzed "Window Ledge" Reactions. *Acc Chem Res*. 2016;49(10):2232-2242.

4. Texier I, Delaire JA, Giannotti C. Reactivity of the charge transfer excited state of sodium decatungstate at the nanosecond time scale. *Phys Chem Chem Phys*. 2000;2(6):1205-1212.

5. Tanielian C. Decatungstate photocatalysis. *Coord Chem Rev*. 1998;178-180:1165-1181.

6. Tanielian C, Cougnon F, Seghrouchni R. Acetone, a substrate and a new solvent in decatungstate photocatalysis. *J Mol Catal Chem*. 2007;262(1-2):164-169.

7. Tanielian C, Seghrouchni R. Decatungstate photocatalyzed oxygenation of methanol in acetonitrile under photostationary state conditions. *Comptes Rendus Chim*. 2014;17(7-8):832-838.

8. Waele VD, Poizat O, Fagnoni M, Bagno A, Ravelli D. Unraveling the Key Features of the Reactive State of Decatungstate Anion in Hydrogen Atom Transfer (HAT) Photocatalysis. *ACS Catal*. 2016;6(10):7174-7182.

9. Duncan DC, Fox MA. Early Events in Decatungstate Photocatalyzed Oxidations: A Nanosecond Laser Transient Absorbance Reinvestigation. *J Phys Chem A*. 1998;102(24):4559-4567.

10. Dondi D, Fagnoni M, Albini A. Tetrabutylammonium Decatungstate-Photosensitized Alkylation of Electrophilic Alkenes: Convenient Functionalization of Aliphatic C-H Bonds. *Chem – Eur J*. 2006;12(15):4153-4163.

11. Tanielian C, Schweitzer C, Seghrouchni R, Esch M, Mechin R. Polyoxometalate sensitization in mechanistic studies of photochemical reactions: The decatungstate anion as a reference sensitizer for photoinduced free radical oxygenations of organic compounds. *PhotochemPhotobiol Sci*. 2003;2(3):297-305.

12. Capaldo L, Bonciolini S, Pulcinella A, Nuño M, Noël T. Modular allylation of C (sp^3)–H bonds by combining decatungstate photocatalysis and HWE olefination in flow. *Chem Sci*. 2022;13(24):7325-7331.

13. Didaratаee S, Suprun A, Joshi N, Scaiano JC. NIR phosphorescence from decatungstate anions allows the conclusive characterization of its elusive excited triplet behaviour and kinetics. *Chem Commun*. 2024;60(14):1896-1899.

14. Bregnhøj M, Westberg M, Jensen F, Ogilby PR. Solvent-dependent singlet oxygen lifetimes: temperature effects implicate tunneling and charge-transfer interactions. *Phys Chem Chem Phys*. 2016;18(33):22946-22961.

15. Hasebe N, Suzuki K, Horiuchi H, et al. Absolute Phosphorescence Quantum Yields of Singlet Molecular Oxygen in Solution Determined Using an Integrating Sphere Instrument. *Anal Chem*. 2015;87(4):2360-2366.

16. Turro NJ. *Modern Molecular Photochemistry*. University science books; 1991. Accessed May 7, 2024.

17. Thorning F, Henke P, Ogilby PR. Perturbed and Activated Decay: The Lifetime of Singlet Oxygen in Liquid Organic Solvents. *J Am Chem Soc*. 2022;144(24):10902-10911.

18. Yamase T, Usami T. Photocatalytic dimerization of olefins by decatungstate (VI),$[W_{10}O_{32}]^{4-}$, in acetonitrile and magnetic resonance studies of photoreduced species. *J Chem Soc Dalton Trans*. 1988;(1):183-190.

19. Lykakis IN, Tanielian C, Seghrouchni R, Orfanopoulos M. Mechanism of decatungstate photocatalyzed oxygenation of aromatic alcohols: part II. Kinetic isotope effects studies. *J Mol Catal Chem*. 2007;262(1-2):176-184.

20. Wan T, Capaldo L, Laudadio G, et al. Decatungstate-Mediated C(sp^3)–H Heteroarylation via Radical-Polar Crossover in Batch and Flow. *Angew Chem Int Ed*. 2021;60(33):17893-17897.

21. Garner A, Wilkinson F. Laser photolysis studies of the triplet state of xanthone and its ketyl radical in fluid solution. *J Chem Soc Faraday Trans 2 Mol Chem Phys*. 1976;72:1010-1020.

22. Neckers DC. Rose bengal. *J PhotochemPhotobiol Chem*. 1989;47(1):1-29.

3.5 Appendix

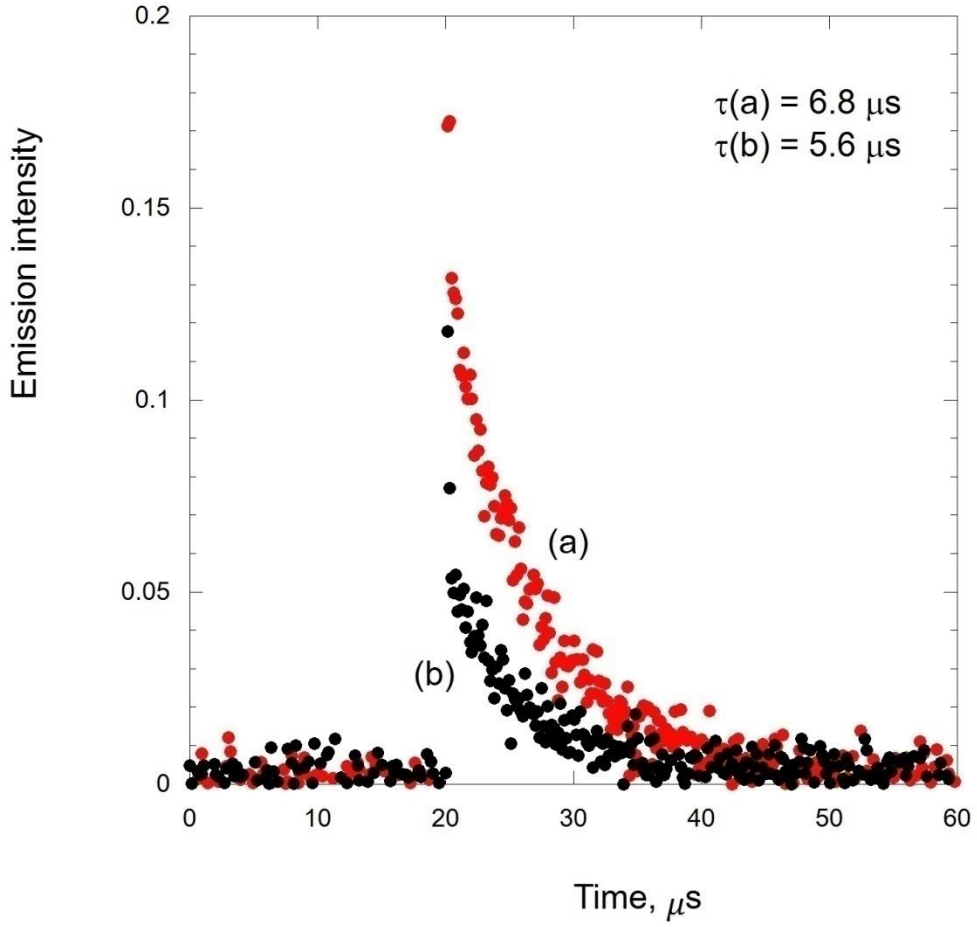

Figure 3.5.1: Decay kinetics at 77K monitored at 1330 nm for a fresh sample (a) and for a sample exposed to ~200 laser shots (b), laser wavelength is 355 nm.

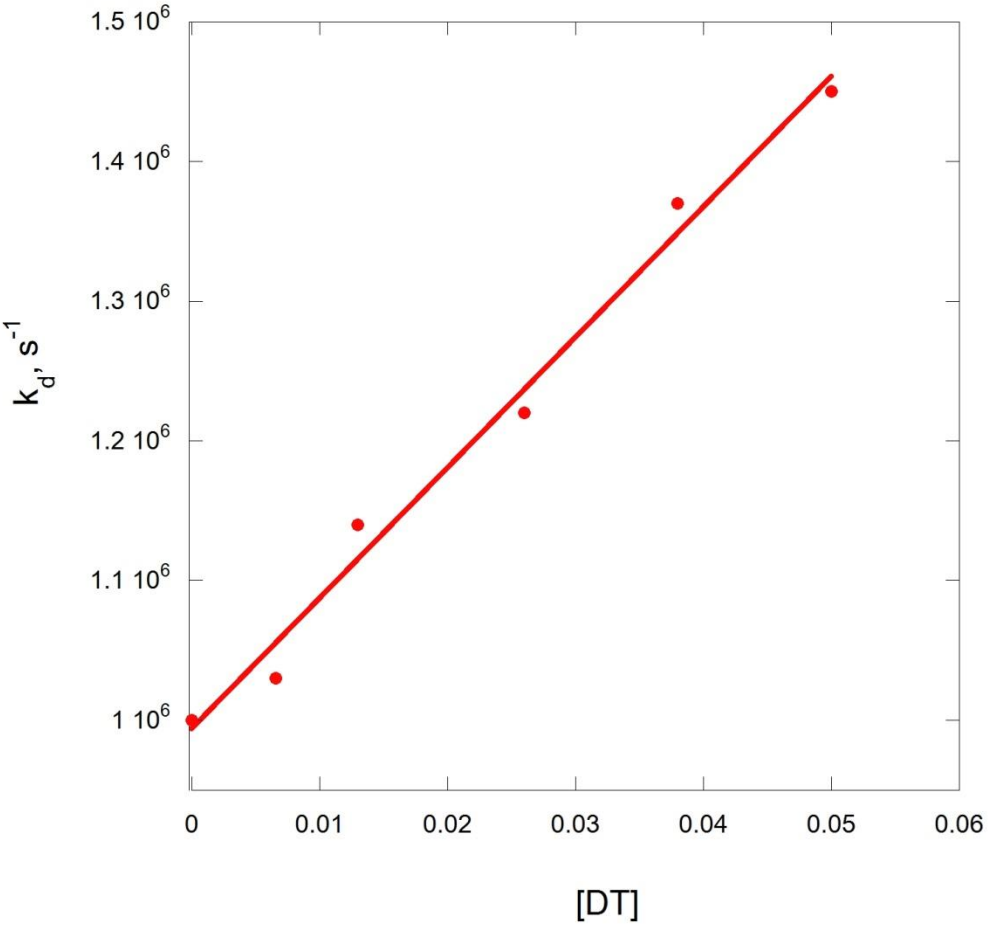

Figure 3.5.2: The slope corresponds to quenching Xanthone by DT, rate constant k_q = 9.3 x 10^9 $M^{-1}s^{-1}$.

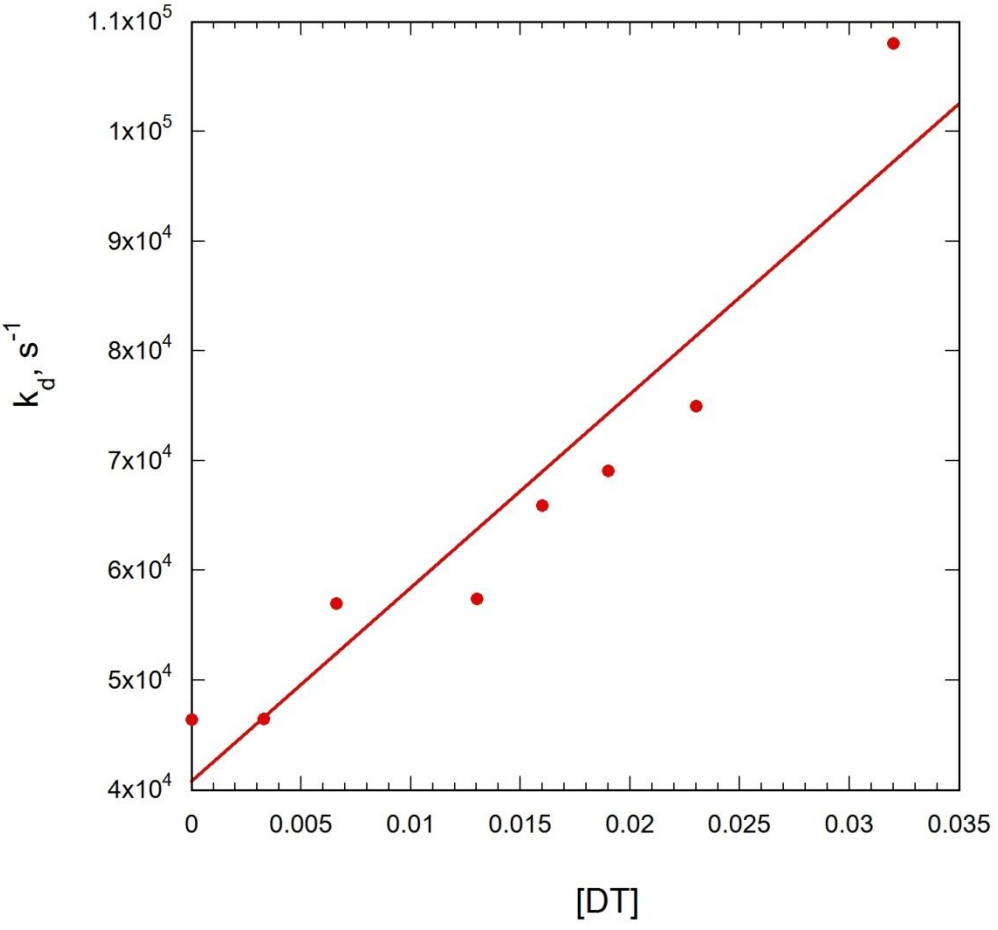

Figure 3.5.3: The slope corresponds to quenching Rose Bengal by DT, rate constant k_q = 1.8 x 10^9 $M^{-1}s^{-1}$.

Chapter 4: Decatungstate triplet quenching by peroxides

4.1 Introduction

There are numerous reports on the application of decatungstate in selectively activating and functionalizing aliphatic compounds at activated C–H positions. This includes benzylic[1], allylic[2], aldehyde C–H bonds[3], and α to ethers[4,5]. An interesting article was published describing a novel method for the direct conversion of aliphatic amines to ketone products via oxidation of a methylene group, using decatungstate as a photosensitizer and hydroperoxide as the terminal oxidant[6]. But we wondered whether the peroxide might have quenched the decatungstate before it reacted with the pyrrolidine, resulting in a competing reaction.

Photochemists have long been captivated by the quenching behavior of the triplet excited states of a photosensitizer by peroxides and hydroperoxides[7–9]. This fascination stems from the potential to glean mechanistic insights into the quenching phenomenon of triplet states. The application of quenching of triplet states by peroxides and hydroperoxide mechanisms spans a wide range of fields. These compounds have been shown to quench excited triplet states, thereby preventing the formation of harmful reactive oxygen species (ROS) such as singlet oxygen[9,10]**.** By quenching excited triplet states and scavenging ROS, these compounds help maintain cellular redox balance and protect against oxidative damage to biomolecules such as proteins, lipids, and DNA[11]. Peroxides and hydroperoxides can scavenge reactive oxygen species (ROS) generated by photosensitized reactions[12,13].

Further, it is worth mentioning that DT-catalyzed oxidations have been found to use oxygen as the primary oxidant. However, studies have also explored the potential of hydroperoxides as a sole oxidant or in combination with oxygen[6]. Despite this, there is still a lack of understanding regarding the kinetics of the interactions between ^{3}DT* or wO and peroxides and hydroperoxides. Therefore, further research is needed to determine the mechanisms and kinetics involved in the reaction of wO with peroxides and hydroperoxides. The rate constant obtained from such investigation can help in deciphering the critical steps in competing photocatalytic reactions involving DT as a photocatalyst.

In this chapter, we examined and compared the quenching behavior of the first excited triplet state of Decatungstate (DT) using various peroxides, namely cumene hydroperoxide, tert-butyl hydroperoxide and hydrogen peroxide. The structures of used quenchers are shown in Figure 4.1.1.

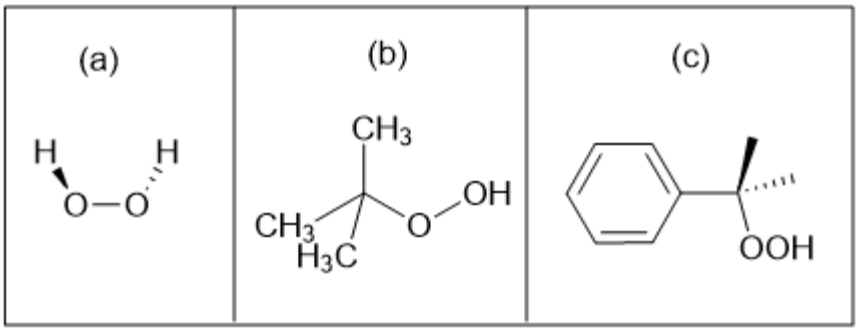

Figure 4.1.1: The structure of hydrogen peroxide (a), tert-butyl hydroperoxide (b) and cumene hydroperoxide (c).

Based on our experimental results and observations and in light of already proposed theories for triplet quenching, we shed light on the mechanism of

triplet quenching of DT by peroxides. In this chapter we use time resolved NIR luminescence to determine these important rate constants.

4.2 Results and discussion

We measured the quenching of decatungstate triplet by three different peroxides (Figure 4.2.1). A solution of 0.2 mM sodium decatungstate in 1:1 ACN:H_2O was prepared. The peroxides were added in portions to the cuvette with NaDT solution, and the emission was monitored at 1330 nm. Following the absorption profile of the DT, the laser excitation with 355 nm was chosen for the present study. For the quenchers we used, no significant absorption at 355 nm was noticed. The quenching constants can be found in Table 4.2.1.

R	DT	Solvent	k,$10^7 M^{-1}s^{-1}$
cumene hydroperoxide	NaDT	1:1 $CH_3CN:H_2O$	126
tert-butyl hydroperoxide	NaDT	1:1 $CH_3CN:H_2O$	9.67
hydrogen peroxide	NaDT	1:1 $CH_3CN:H_2O$	3.71

Table 4.2.1: Rate constants for reaction of ^{3}DT* with different peroxides.

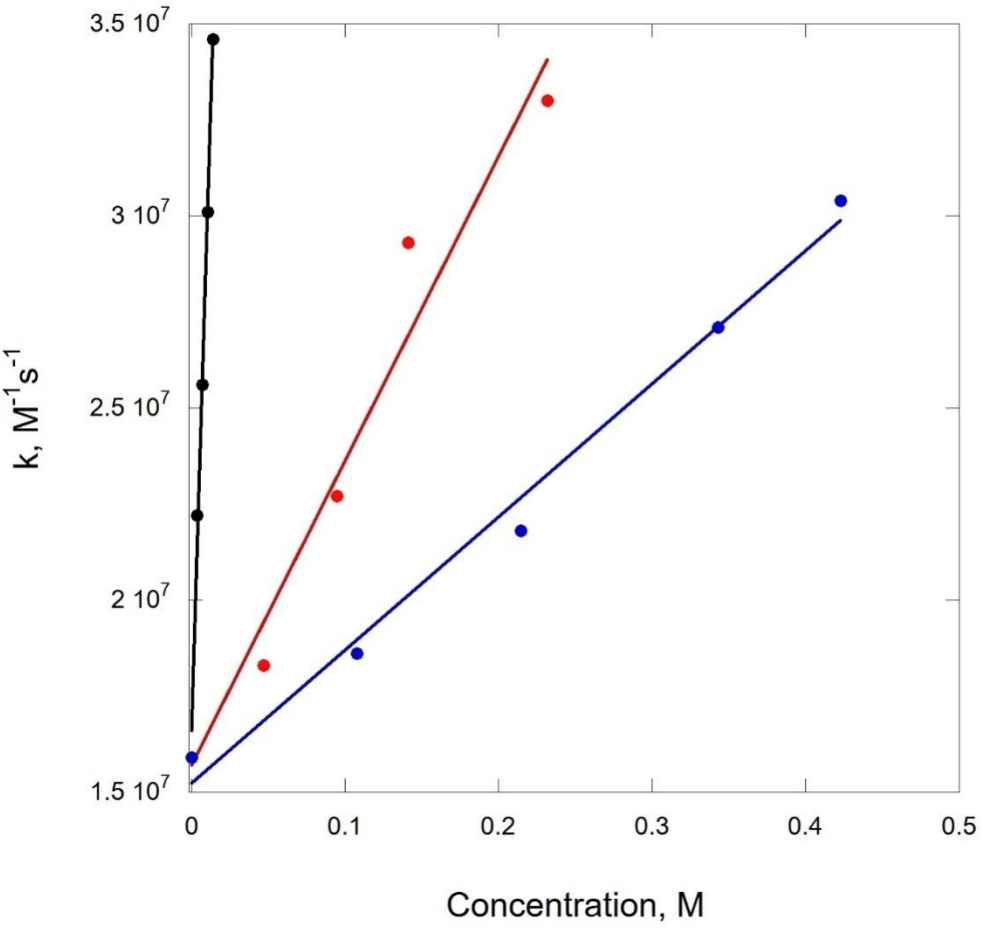

Figure 4.2.1: Quenching for NaDT in 1:1 acetonitrile:H_2O at room temperature for three peroxides: cumene hydroperoxide (black), tert-Butyl hydroperoxide (red) and hydrogen peroxide (blue). Data are based on emission kinetics monitored at 1330 nm.

Figure 4.2.2 shows the quenching of the phosphorescence decay of DT by cumene hydroperoxide, (decays for two other quenchers are in appendix). Similar quenching behavior was observed with other quenchers. From Table 4.2.1, it is clear that the quenching rates are higher for hydroperoxides in

comparison to hydrogen peroxide; this is associated with hygrogen bonding, which makes it harder to abstract hydrogen from peroxide.

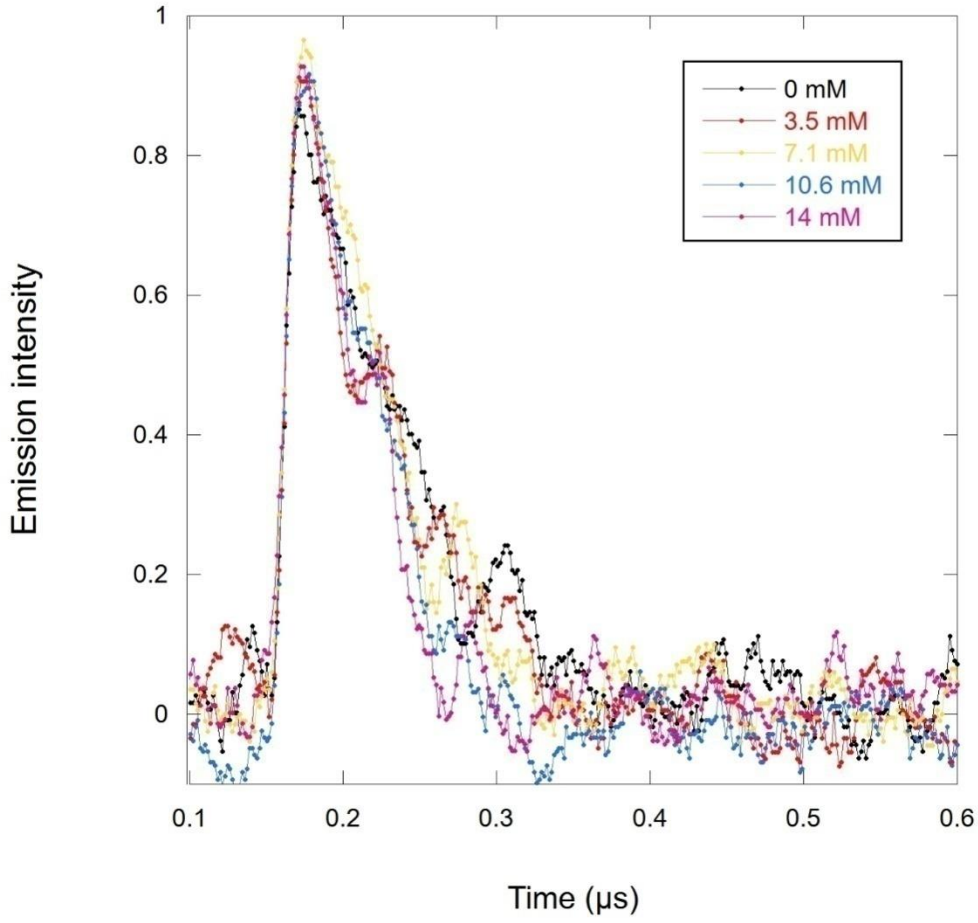

Figure 4.2.2: Quenching for NaDT in 1:1 acetonitrile:H_2O at room temperature by cumene hydroperoxide of different total concentrations: 0 mM (black) 3.5 mM (red), 7.1 mM (yellow), 10.6 mM (blue), 14 mM (purple); emission was monitored at 1330 nm following 355 nm laser excitation.

The experimental rate constant or triplet decay, k_{exp}, can be related to the bimolecular rate constant for triplet quenching, k_q, according to eq. 1.

$$k_{exp} = k_0 + k_q[Q] \quad (1)$$

Where, k_0 is the first-order rate constant for triplet decay in the absence of quencher (Q) and in the plot corresponds to the interception the y-axis.

As mentioned in the introduction, the quenching analysis of wO with peroxides and hydroperoxide can help explain why, as quenchers of wO, peroxide and hydroperoxide may serve as co-catalysts in a photocatalytic reaction.

The activation of C-H bonds via oxidation has been investigated in the presence of hydroperoxides[6]. The study found that hydrogen peroxide was a more effective co-catalyst than tert-butyl hydroperoxide. These results are surprising and exciting, as our quenching experiments (Table 4.2.1) demonstrate that hydrogen peroxide is the slowest quencher for ^{3}DT*.

Although we note that the quenchers under investigations are relatively good quenchers, in our research group, Julia Ong, investigated the effect of H_2O_2 in conjunction with O_2 for the photooxidation of 1-phenylethanol. The chemical structure of 1-phenylethanol in Figure 4.2.3 (3). Her results show that H_2O_2 has a significant effect in the early stages of the reaction, but its impact diminishes as the reaction progresses.

Our kinetic studies show that hydroperoxides are excellent quenchers of ^{3}DT*, and the results support HAT as the quenching mechanism. Thus, reaction of DT with hydrogen peroxide (Figure 4.2.3 (2)) is expected to

quench, yielding two of the intermediates already involved in the oxidation of 1-phenylethanol and 1,4-cyclohexadiene(Figure 4.2.3)**.**

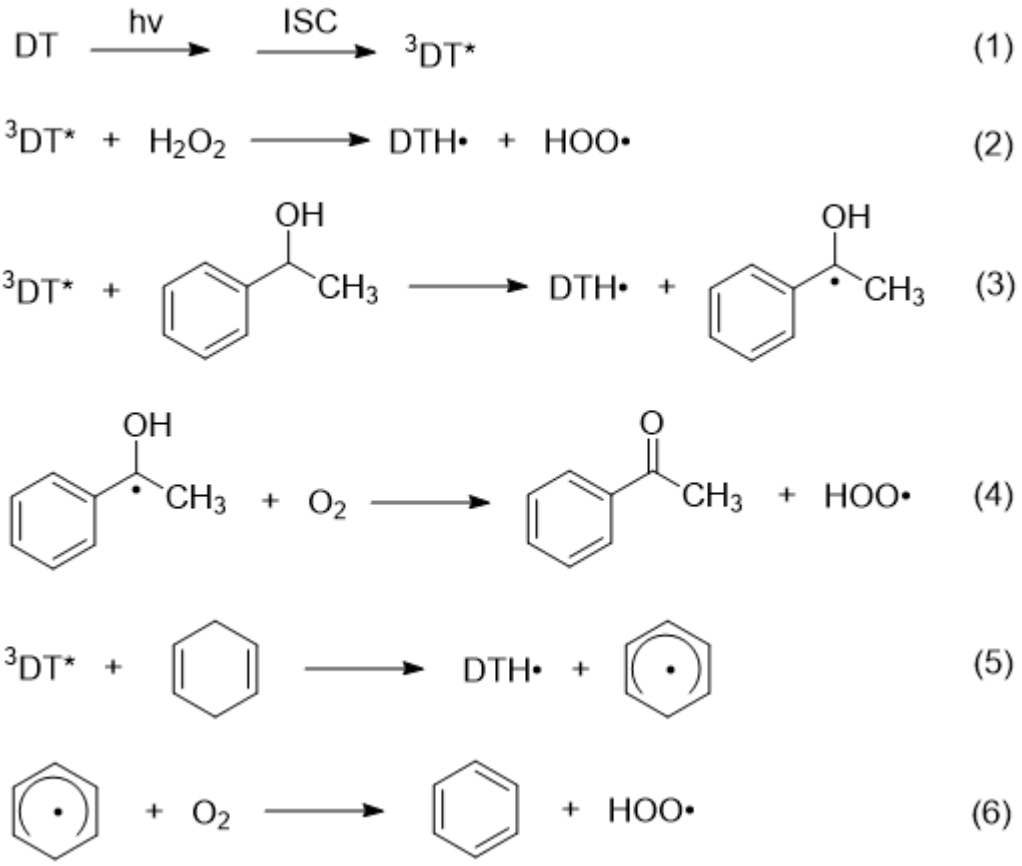

Figure 4.2.3: The proposed mechanism for HAT and the subsequent reaction of the radicals with oxygen: (1) – decatunstate photoexitation; (2) – reaction of $^3DT^*$ with hydrogen peroxide; (3) – reaction of $^3DT^*$ with 1-phenylethanol; (4) – reaction of 1-phenylethanol radical with oxygen; (5) - reaction of $^3DT^*$ with 1,4-cyclohexadiene; (6) - reaction of 1,4-cyclohexadienyl radical radical with oxygen.

Given that DTH• and HOO• are already generated through the proposed mechanism, we wondered how the addition of H_2O_2 could facilitate C-H activation. The lifetime for $^3DT^*$ in the water-rich solvent used can be estimated as 40 ns. With a rate constant for 1-phenylethanol of 1.5 x 10^8M^-

$^1s^{-1}$. Our calculation suggests that the fraction of DT triplets quenched by 1-phenylethanol can be calculated with equation 2.

$$f_Q = \text{fraction quenched} = \frac{k_Q \times [Q]}{\tau^{-1} + k_Q \times [Q]} = \frac{1.5 \times 10^8 \times 0.1}{2.5 \times 10^7 + 1.5 \times 10^8 \times 0.1}$$

$$= 0.375(2)$$

That is, only 37.5% of the DT triplets are quenched by the concentration of 1-phenylethanol used. Thus, adding hydrogen peroxide, a good ^{3}DT* quencher, will increase the fraction of ^{3}DT* that can generate reaction intermediates. Beyond this it is necessary to establish is DTH• and HOO•, generated in reaction (2) are also capable or promoting the oxidation of 1-phenylethanol or 1,4-cyclohexadiene. In the presence of two quenchers (both, 1-phenylethanol and H_2O_2), the equation changes as shown below, giving $\boldsymbol{f}_{QQ}$= 0.573 for 0.5M H_2O_2, that is, more triplets are quenched when 0.5 H_2O_2 M is present.

$$f_{QQ} = \text{fraction quenched} = \frac{k_Q \times [Q] + k_{H2O2} \times [H_2\,O_2\,]}{\tau^{-1} + k_Q \times [Q] + k_{H2O2} \times [H_2\,O_2\,]}$$

$$= \frac{1.5 \times 10^8 \times 0.1 + 3.71 \times 10^7 \times 0.5}{2.5 \times 10^7 + 1.5 \times 10^8 \times 0.1 + 3.71 \times 10^7 \times 0.5}$$

$$= 0.573(3)$$

The efficiency of the reaction will decrease as both concentration terms are reduced during the progress of the oxidation. The efficiency can be increased slightly by replacing water with D_2O, where the ^{3}DT* lifetime is roughly twice as long[14].

Regarding the reactivity of DTH• and HOO•, Figure 4.2.4 suggests the reactions that may be involved including reactions 7 and 8 where DTH• transfers hydrogen atom (or electron) to the peroxide bond in Fenton-like chemistry (Figure 4.2.4 (9) and (10)).

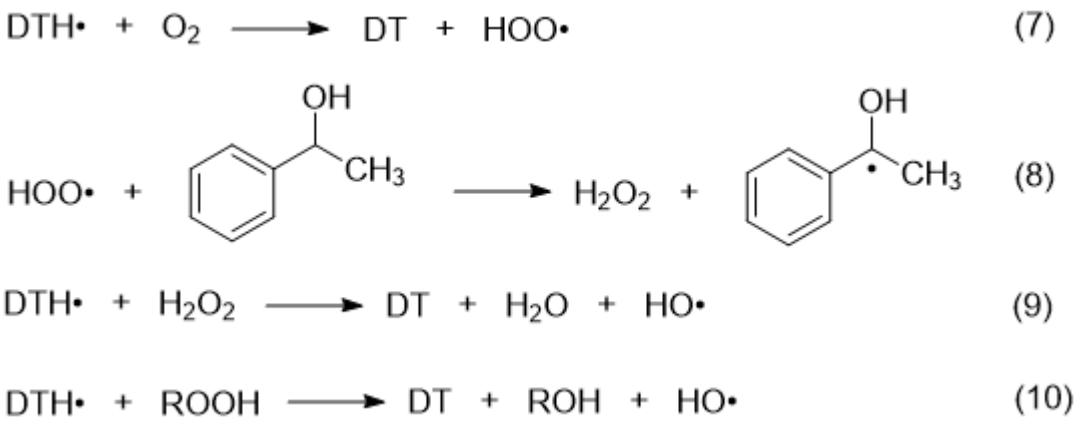

Figure 4.2.4: Reactions that may be involved due to a reactivity of DTH• and HOO•: (7) – reaction of DTH• with oxygen; (8) – reaction of HOO• with 1-phenylethanol; (9) – reaction of DTH• with hydrogen peroxide; (10) - reaction of DTH• with hydroperoxide.

That some of these reactions must be taking place is unequivocally demonstrated by the fact that addition of hydrogen peroxide increases the initial rate of oxidation. Further, the intermediates involved are capable of propagating a chain reaction as illustrated in Figure 4.2.5 for the case of 1,4-cyclohexadiene.

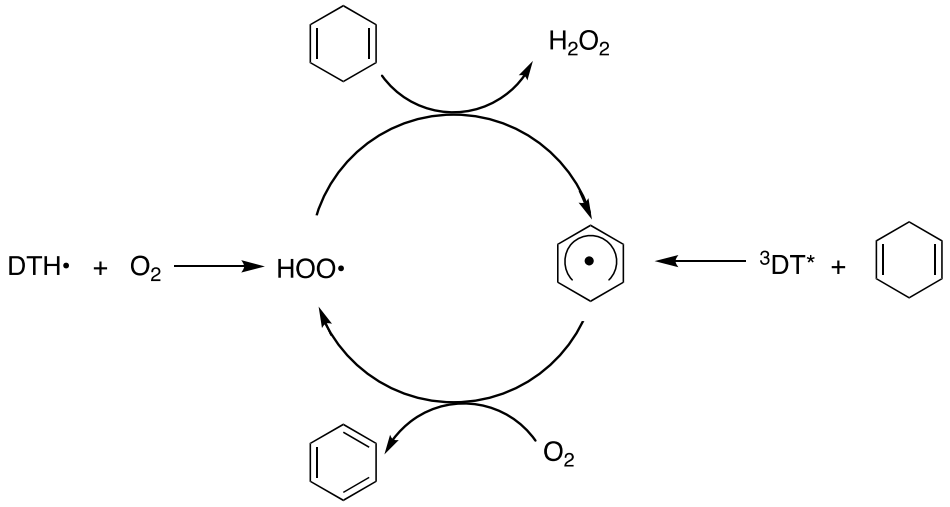

Figure 4.2.5: Proposed chain reaction for 1,4-cyclohexadiene in the presence of oxygen (no hydroperoxides) where DTH• can act as an initiator via reaction (7). Similarly, reaction (5) can feed directly the chain by supplying cyclohexadienyl radicals. In the presence of hydroperoxides, additional peroxyl radicals and DTH• would be formed via reaction (7).

While Figure 4.2.5 shows a viable chain reaction, we may wonder if it actually occurs, particularly considering that the initiation via ^{3}DT* HAT reactions with 1-phenylethanol or 1,4-cyclohexadiene are much faster than typical HAT reactions involving peroxyl radical attack on C-H bonds. For example, HOO• reacts with 1,4-cyclohexadiene with a rate constant of 350 $M^{-1}s^{-1}$ in acetonitrile[15], compared with 3.0 x $10^8 M^{-1}s^{-1}$ for ^{3}DT*[14]; hydroperoxyl rate constants are also very solvent dependent[15].

We can easily calculate which is the minimum quantum yield to support a chain reaction. We know that ^{3}DT* is formed with a quantum yield of 0.6[16] and that only 37.5% of the triplets are quenched by 0.1M 1-phenylethanol.

$$Primary\Phi \text{ of radical formation} = \Phi_R = \Phi_{ISC} x f_Q = 0.6 \text{ x} 0.375$$
$$= 0.225(4)$$

Since quantum yields measured exceed 0.225, then a chain is required, likely a short chain, but enough to support the mechanism of Figure 3.2.5. The value of quantum yield for 1-phenylethanol $\boldsymbol{\Phi}_R = 0.93 \pm 0.10$, suggests a chain length of at least 5. There is also evidence that oxidative C-H oxidations work better under oxygen than under air. This suggests that reactions (5), (6) or (7) may not be quantitative under air, somewhat surprising given the fast rate constants that characterize radical trapping by oxygen[17]. With H_2O_2 the triplet DT capture triples, the product yield increases.

$$Primary\Phi \text{ of radical formation} = \Phi_R = \Phi_{ISC} x f_{QQ} = 0.6 \text{ x} 0.573$$
$$= 0.344(5)$$

4.3 Conclusions

In this chapter, we illustrate the quenching of decatungstate triplet by three different peroxides, the rates of quenching range from 10^9 to $10^7 M^{-1}s^{-1}$. The insights gained from our study are essential for developing new and effective strategies for harnessing the potential of DT in various applications.

4.4 References

1. Qrareya H, Ravelli D, Fagnoni M, Albini A. Decatungstate Photocatalyzed Benzylation of Alkenes with Alkylaromatics. *Adv Synth Catal*. 2013;355(14-15):2891-2899.

2. Lykakis IN, Orfanopoulos M. *Lone* Selectivity of the Decatungstate-Sensitized Photooxidation of 1-Substituted Cycloalkenes. *Synlett*. 2004;(12):2131-2134.

3. Esposti S, Dondi D, Fagnoni M, Albini A. Acylation of electrophilic olefins through decatungstate-photocatalyzed activation of aldehydes. *Angew Chem-Int Ed Engl-*. 2007;46(14):2531.

4. Ravelli D, Zoccolillo M, Mella M, Fagnoni M. Photocatalytic Synthesis of Oxetane Derivatives by Selective C□H Activation. *Adv Synth Catal*. 2014;356(13):2781-2786.

5. Ryu I, Tani A, Fukuyama T, Ravelli D, Montanaro S, Fagnoni M. Efficient C–H/C–N and C–H/C–CO–N Conversion via Decatungstate-Photoinduced Alkylation of Diisopropyl Azodicarboxylate. *Org Lett*. 2013;15(10):2554-2557.

6. Schultz DM, Lévesque F, DiRocco DA, et al. Oxyfunctionalization of the Remote C−H Bonds of Aliphatic Amines by Decatungstate Photocatalysis. *Angew Chem Int Ed*. 2017;56(48):15274-15278.

7. Ingold KU, Johnston LJ, Lusztyk J, Scaiano JC. Triplet quenching by diacyl peroxides. *Chem Phys Lett*. 1984;110(4):433-436.

8. Ng HC, Guillet JE. Photochemistry of Ketone Polymers. 13. Quenching of Excited Ketone Carbonyls by Hydroperoxides and Peroxides. *Macromolecules*. 1978;11(5):937-942.

9. Engel PS, Woods TL, Page MA. Quenching of excited triplet sensitizers by organic peroxides. *J Phys Chem*. 1983;87(1):10-13.

10. Urano T, Kitamura A, Sakuragi H, Tokumaru K. Quenching of excited singlet states by dibenzoyl peroxide and *tert*-butyl peroxybenzoate. *J Photochem*. 1984;26(1):69-73. doi:10.1016/0047-2670(84)85028-5

11. Finkel T, Holbrook NJ. Oxidants, oxidative stress and the biology of ageing. *Nature*. 2000;408(6809):239-247.

12. Scaiano JC, Wubbels GG. Photosensitized dissociation of di-tert-butyl peroxide. Energy transfer to a repulsive excited state. *J Am Chem Soc*. 1981;103(3):640-645.

13. Stewart LC, Carlsson DJ, Wiles DM, Scaiano JC. Triplet quenching by tert-butyl hydroperoxide. *J Am Chem Soc*. 1983;105(11):3605-3609.

14. Didaratаee S, Suprun A, Joshi N, Scaiano JC. NIR phosphorescence from decatungstate anions allows the conclusive characterization of its elusive excited triplet behaviour and kinetics. *Chem Commun*. 2024;60(14):1896-1899.

15. Howard JA, Ingold KU. Absolute rate constants for hydrocarbon autoxidation. V. The hydroperoxy radical in chain propagation and termination. *Can J Chem*. 1967;45(8):785-792.

16. Tanielian C. Decatungstate photocatalysis. *Coord Chem Rev*. 1998;178:1165-1181.

17. Maillard B, Ingold KU, Scaiano JC. Rate constants for the reactions of free radicals with oxygen in solution. *J Am Chem Soc*. 1983;105(15):5095-5099.

4.5 Appendix

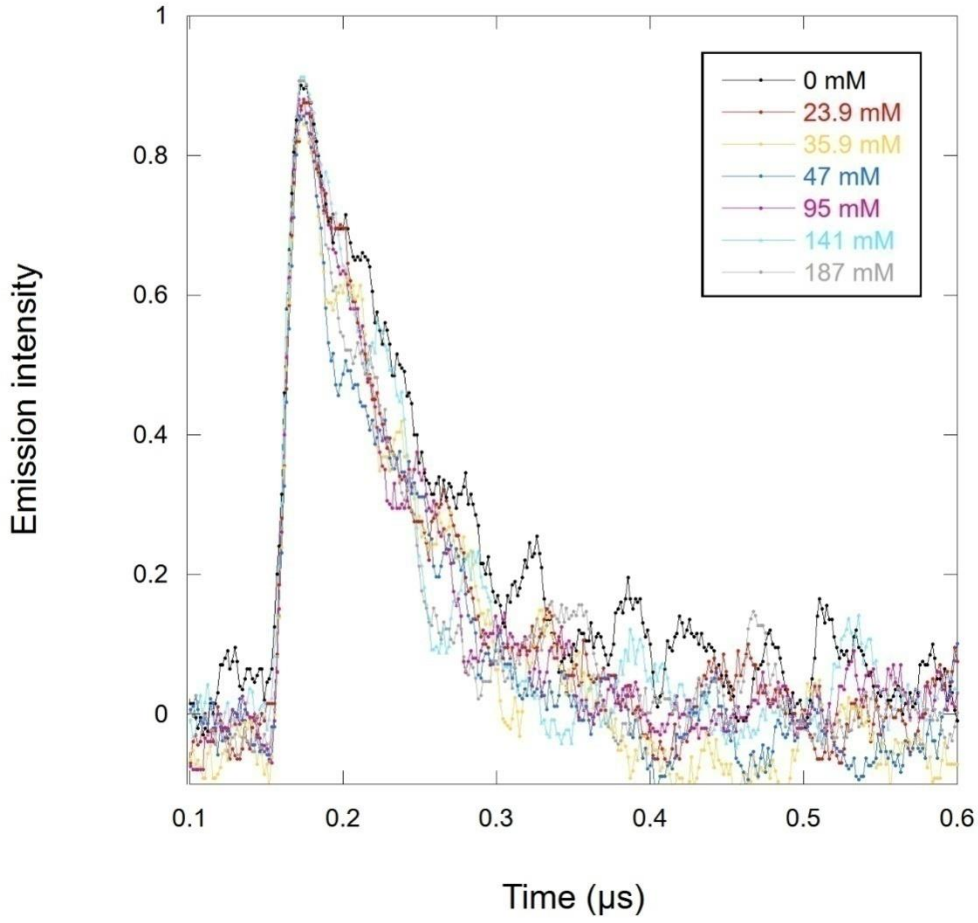

Figure 4.5.1: Quenching for NaDT in 1:1 acetonitrile:H_2O at room temperature by tert-Butyl hydroperoxide of different total concentrations: 0mM (black), 23.9 mM (red), 35.9 mM (yellow), 47mM (blue), 95mM (purple),141mM (light blue),187mM (gray); emission was monitored at 1330 nm following 355 nm laser excitation.

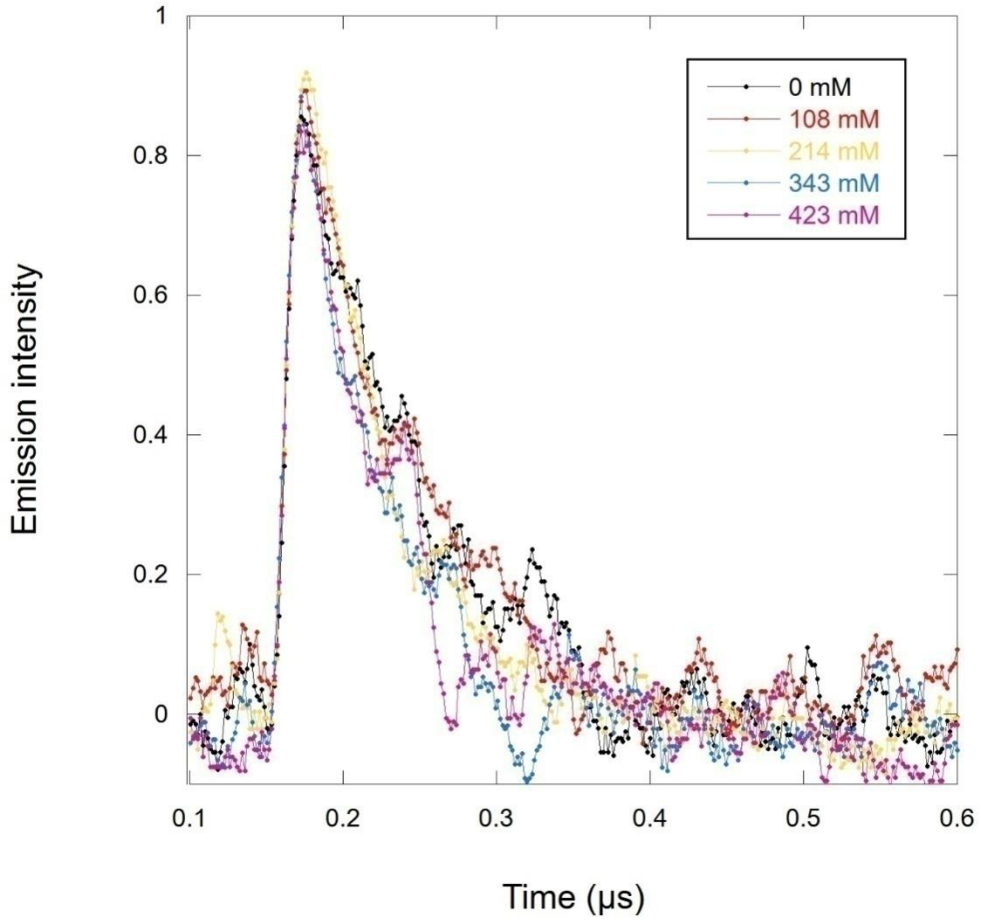

Figure 4.5.2: Quenching for NaDT in 1:1 acetonitrile:H_2O at room temperature by hydrogen peroxide of different total concentrations: 0mM (black) 108 mM (red), 214 mM (yellow), 343 mM (blue), 423 mM (purple); emission was monitored at 1330 nm following 355 nm laser excitation.

Chapter 5: Future Directions

In this work the DT intermediate wO was shown to be a triplet, what opens up many directions for further research in this area. Investigations of such important data as rate constants for different quenchers will allow to better understand the mechanisms of reaction which includes DT as a photocatalyst.

The quenching of ^{3}DT* with hydroperoxides shed light on the photooxidation of 1-phenyl ethanol in the presence of hydrogen peroxide and help explain why H_2O_2 has a significant effect in the early stages of the reaction but decrease as the reaction progresses. As addition of hydrogen peroxide increases the initial rate of oxidation, the intermediates involved are capable of propagating a chain reaction.

Decatungstate has shown potential in reactions involving hydrogen atom transfer (HAT) mechanisms. Decatungstate ($[W_{10}O_{32}]^{4-}$) is a powerful photocatalyst known for its ability to activate a wide range of substrates through single-electron transfer processes and can be a good choice to induce polarity reversal in various organic substrates. Polarity reversal catalysis is a concept in organic chemistry where a catalyst reverses functional group or molecule's inherent reactivity (or polarity). This technique of catalysis to facilitate the use of radicals from electron-poor substrates. The basis of polarity-reversal catalysis (PRC) is to replace a single-step abstraction, which is slow, with a two-step process mediated by radicals which is faster. Polarity reversal catalysis is a promising approach for selective oxidation reactions, where the oxidation state of a substrate is reversed.

The oxidation of benzyl alcohol to benzaldehyde using decatungstate under light irradiation involves several steps (Figure 5.1). These steps primarily feature the formation of radicals through hydrogen atom transfer (HAT). The process involves the excitation of decatungstate by light, facilitating the hydrogen atom transfer from benzyl alcohol, forming a benzyl radical. This radical subsequently oxidizes to produce benzaldehyde, while decatungstate is regenerated, completing the catalytic cycle. The role of decatungstate is crucial as it acts both as a catalyst and facilitator of the hydrogen atom transfer process, making the overall reaction efficient and selective.

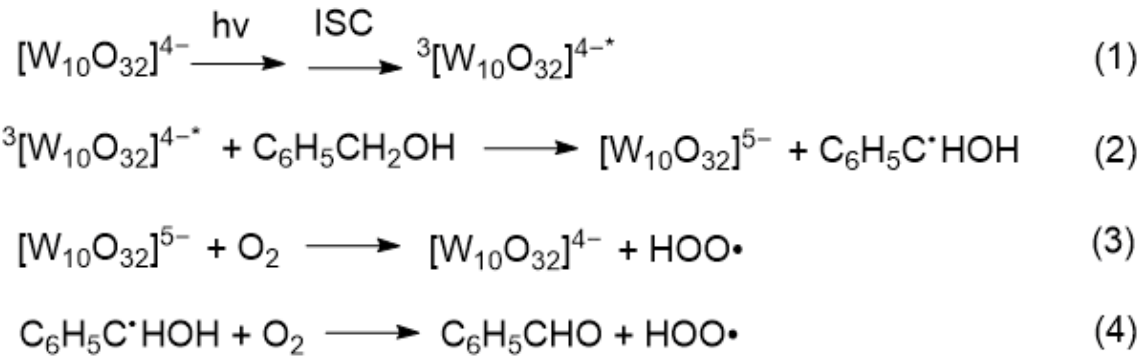

Figure 4.5.1: The oxidation of benzyl alcohol to benzaldehyde: (1) – photoexitation of decatungstate; (2) - reaction of $^{3}DT^{*}$ with benzyl alcohole; (3) - reaction of DTH• with oxygen; (4) – reaction of benzyl radical with oxygen.

This investigation will show the advanced capabilities of decatungstate and laser flash photolysis to unlock new avenues in polarity reversal catalysis, offering significant advancements in synthetic chemistry. The findings will deepen understanding of decatungstate's catalytic capabilities and expand the toolbox for synthetic chemists, facilitating the creation of novel compounds and materials.